

The C-terminal extension landscape of naturally presented HLA-I ligands

Running title: C-terminal extensions in HLA-I ligands.

Philippe Guillaume^a, Sarah Picaud^{b,c}, Petra Baumgaertner^a, Nicole Montandon^a, Julien Schmidt^a, Daniel E Speiser^a, George Coukos^a, Michal Bassani-Sternberg^a, Panagis Fillipakopoulos^{b,c}, David Gfeller^{a,d,1,2}

^aLudwig Institute for Cancer Research, Department of Fundamental Oncology, University of Lausanne, 1066 Epalinges, Switzerland.

^bStructural Genomics Consortium, Old Road Campus Research Building, Roosevelt Drive, Nuffield Department of Clinical Medicine, University of Oxford, Roosevelt Drive, Oxford OX3 7DQ, UK.

^cLudwig Institute for Cancer Research, Nuffield Department of Clinical Medicine, University of Oxford, Roosevelt Drive, Oxford OX3 7DQ, UK.

^dSwiss Institute of Bioinformatics (SIB), 1015 Lausanne, Switzerland.

¹ To whom correspondence should be addressed: David.Gfeller@unil.ch.

² D.G. should be considered both as first and last author.

Abstract

HLA-I molecules play a central role in antigen presentation. They typically bind 9- to 12-mer peptides and their canonical binding mode involves anchor residues at the second and last positions of their ligands. To investigate potential non-canonical binding modes we collected in-depth and accurate HLA peptidomics datasets covering 54 HLA-I alleles and developed novel algorithms to analyze these data. Our results reveal frequent (442 unique peptides) and statistically significant C-terminal extensions for at least eight alleles, including the common HLA-A03:01, HLA-A31:01 and HLA-A68:01. High resolution crystal structure of HLA-A68:01 with such a ligand uncovers structural changes taking place to accommodate C-terminal extensions and helps unraveling sequence and structural properties predictive of the presence of these extensions. Scanning viral proteomes with the new C-terminal extension motifs identifies many putative epitopes and we demonstrate direct recognition by human CD8⁺ T cells of a 10-mer epitope from cytomegalovirus predicted to follow the C-terminal extension binding mode.

Significance

HLA-I molecules play a central role in immune recognition of infected or cancer cells. They bind short intracellular peptides of 9 to 12 amino acids and present them to T cell for immune recognition. For many years the length restriction of HLA-I ligand has been a central dogma in antigen presentation. Combining analysis of Mass Spectrometry data with novel algorithms, X-ray crystallography and T cell recognition assays, we show that a substantial fraction of HLA-I molecules bind peptides extending beyond the C-terminus of canonical ligands. As such, our results uncover a new type of CD8 T cell epitopes and our ability to accurately predict them will help studying their role in infectious diseases or cancer immunotherapy.

\body

Introduction

Human Leukocyte Antigen class I (HLA-I) molecules play a major role in immune defense mechanisms by presenting to T cells peptides from the intracellular matrix. Peptides presented on HLA-I molecules originate mainly from proteasomal degradation of self or pathogen-derived proteins. These peptides are first translocated to the endoplasmic reticulum. There, they can load on HLA-I molecules provided their sequence is compatible with HLA-I binding motifs. Peptide-HLA-I complexes are then transported to the cell surface where they can elicit T cell recognition, primarily upon presentation of non-self peptides.

Most HLA-I alleles preferentially bind 9- to 12-mer peptides (1-5) and the majority of alleles accommodate peptides with anchor residues at the second and last positions. From a structural point of view, anchor residues point directly into the HLA-I peptide binding groove. Their importance for HLA-I peptide interactions is also reflected at the sequence level, where alignments of HLA-I ligands display clear specificity at the second and last positions for most alleles. 9-mer HLA-I ligands are characterized by a linear binding mode. For longer peptides, numerous crystal structures have shown the presence of a bulge at middle positions, protruding outside of the HLA-I binding site in order to accommodate the additional residues between the two anchor positions (e.g., ref. (6)).

Over the years, anecdotal evidences of C-terminal extensions beyond the last anchor position have been observed among HLA-A02:01 ligands and crystal structures with such ligands were published first in 1994 (7) and later in 2009 (8). More recently, analysis of HLA peptidomics data obtained by Mass Spectrometry (MS) from cell lines transfected with soluble HLA-A02:01 and infected with *Toxoplasma gondii* revealed several C-terminal extensions and showed that, for this allele, C-terminal extensions were mainly found among peptides coming from pathogens (9, 10). X-ray crystallography revealed distinct structural mechanisms in HLA-A02:01 to accommodate C-terminal extensions (9, 10). N-terminal extensions have also been recently observed in HLA-B57:01 (11) and HLA-B58:01 (12). However, N- or C-terminal extensions have not been much investigated in other HLA-I alleles based on unbiased HLA-I ligand datasets (see some predictions in (15, 16), and results in

mouse (13)). As such, it remains unclear whether they occur frequently and, if yes, whether they can be recognized by CD8 T cells, although the latter may be expected. Here, we introduce a novel statistical approach to rigorously investigate N- and C-terminal extensions in large datasets of naturally presented HLA-I ligands obtained by in depth HLA peptidomics profiling of cell lines and tissue samples covering more than 50 HLA-I alleles. Our work reveals widespread C-terminal extensions for at least eight HLA-I molecules (HLA-A02:03, HLA-A02:07, HLA-A03:01, HLA-A31:01, HLA-A68:01, HLA-A68:02, HLA-B27:05 and HLA-B54:01), and we identify both sequence and structural features in HLA-I alleles predictive of the presence of C-terminal extensions. A new crystal structure of HLA-A68:01 in complex with such a ligand uncovers structural changes to accommodate the C-terminal extensions. Scanning viral proteomes with our new motifs describing C-terminal extensions further enabled us to demonstrate direct CD8 T cell recognition of an HLA-A03:01 restricted epitope from cytomegalovirus (CMV) predicted to follow the C-terminal extension binding mode.

Results

Unbiased investigation of C- and N-terminal extensions

To investigate the presence of C- and N-terminal extensions in HLA-I ligands, we collected recent pooled and mono-allelic HLA peptidomics datasets from seven studies covering 43 samples, 54 different HLA-I alleles and 109,953 unique peptides (2, 14-19) (SI Appendix and Dataset S1). These datasets were all generated with <1% false discovery rate and were not filtered with any predictor. We hypothesized that C- or N-terminal extensions among naturally presented endogenous HLA-I ligands may be determined by identifying peptides of ten or more amino acids that do not match motifs expected for ligands following the bulge model (Fig. 1A). For pooled HLA peptidomics data, 9-mer binding motifs were identified and annotated with our recent motif deconvolution algorithm (4, 19) (Fig. 1B and SI Appendix). Importantly, these motifs were identified without relying on HLA-I ligand predictors and therefore represent a fully unbiased view of the binding specificity of HLA-I alleles. Focusing on the first three and the last two positions in the 9-mer motifs, we then built Position Weight Matrices (PWM) modeling bulges, N-terminal extensions or C-terminal

extensions for each of the 9-mer motifs (SI Appendix). For 10-mers, bulges were modeled by incorporating five non-specific positions between the first three and the last two residues. C-, respectively N-, terminal extensions were modeled by adding four non-specific positions in the middle and one non-specific position at the C-, respectively N-terminus (SI Appendix and Fig. 1C).

Using the three models derived from each 9-mer motif, we then scored all 10-mer peptides (Fig. 1C and SI Appendix). Peptides that displayed a significantly higher score for exactly one allele and one model were assigned to this allele and the corresponding model (SI Appendix). For mono-allelic cell lines, comparison was only performed among bulge, N- and C-terminal extension models of the same allele. To determine statistical significance of N- or C-terminal extensions, we developed a null model representing the expected 10-mer HLA-I ligands assuming only bulges (SI Appendix). We finally retrieved all sets of peptides predicted to follow N- or C-terminal extensions associated to a given allele in a given sample that passed statistical significance ($Z\text{-score} > 2$). This resulted in 15 motifs of C-terminal extensions (for a total of 396 unique 10-mer peptides) and no motif of N-terminal extensions (Fig. 2A and S1). Seven motifs corresponded to C-terminal extensions associated to HLA-A03:01 across different samples, two motifs to HLA-A68:01 and one motif to each of the other alleles (i.e., HLA-A02:03, HLA-A02:07, HLA-A31:01, HLA-A68:02, HLA-B27:05 and HLA-B54:01, Fig. 2A, SI Appendix, Fig. S2, Dataset S2 and S3). We first note that motifs describing C-terminal extensions associated to the same allele (i.e., HLA-A03:01 or HLA-A68:01) in different datasets displayed a very high similarity among each other (rectangles in Fig. 2A). This highlights the remarkable reproducibility of our predictions across our very heterogeneous set of HLA peptidomics studies. The average frequency of C-terminal extensions among 10-mer ligands is shown in Fig. 2B.

To investigate whether C-terminal extensions may extend for more than one amino acid, we applied our approach to longer peptides (SI Appendix) and found statistically significant evidences of C-terminal extensions for HLA-A02:07 and HLA-B27:05 for a total of 46 unique 11-mer peptides (Fig. 2C-D, Dataset S2 and S3). The motifs are consistent with the 10-mer C-terminal extensions (Fig. 2A). A trend was also observed in some samples for HLA-A02:01, HLA-A02:03, HLA-A03:01, HLA-A68:02 and HLA-B54:01 (Dataset S2), although it did not pass our thresholds on the number of ligands or the Z-score. When analyzing even longer ligands (12-mers), we

did not find anything statistically significant, but the number of such ligands identified by MS is much smaller so that it may be difficult to confidently identify C-terminal extensions with our approach.

Robustness to noise

To explore the robustness of our findings with respect to noise in HLA peptidomics data, we rerun our whole pipeline adding 5% of randomly selected peptides from the human proteome to all datasets. Remarkably, the predicted C-terminal extensions remained basically unchanged (SI Appendix, Fig. S3). In particular, we did not observe any new C-terminal extension motifs that would arise from the random peptides. This clearly suggests that C-terminal extensions predicted in this work are not resulting from contaminations in HLA peptidomics data.

In vitro validation

To experimentally test our predictions, we selected 10-mer ligands predicted to follow the C-terminal extension binding mode for three alleles (HLA-A03:01, HLA-A31:01, HLA-A68:01). We mutated either the last or second-to-last residue and experimentally measured the stability of the wild-type and the two mutated peptides (SI Appendix). 9-mer peptides without the predicted C-terminal extensions were used as positive controls. As expected mutating the last residue had little effect on their binding stability, while mutating the second to last residue significantly decreased the stability (Fig. 3). These data strongly suggest that, for these peptides, the second to last residue is playing the role of the anchor residue and the last residue is extending beyond the canonical C-terminus of HLA-I ligands. We also tested other P10 mutants that did not match the motif predicted by our analysis. In general, the stability of these mutants was lower than for peptides seen in MS data, especially for HLA-A03:01 and HLA-A68:01 (SI Appendix, Fig. S4). Of note, peptides with R or K at P10 could also form bulges, which likely explains their higher stability. To test whether longer C-terminal extensions may bind to HLA-A03:01, we added all amino acids not compatible with the bulge model at the C-terminus of the 10-mer HLA-A03:01 ligand KLAYTLLNKL and measured the stability of these peptides (SI Appendix, Fig. S5). Our results indicate that most of the 11-mers did bind, although with lower stability compared to the 10-mer peptide. This suggests that longer C-terminal extensions can extend for more than one residue in HLA-A03:01 ligands, although this likely

corresponds to a small fraction of the actual HLA peptidome, as suggested by their low frequency in MS data.

We then analyzed peptides that displayed similar scores for the bulge and the C-terminal extension model (red circles in SI Appendix, Fig. S1). Most of them displayed the same or very similar amino acids at P9 and P10 (Dataset S4). To investigate whether they are more likely to adopt a bulge or a C-terminal extension binding mode, we measured the stability of RYIEIFPSRR with HLA-A31:01. R(9)S did not affect the binding, while R(10)S decreased the stability (SI Appendix, Fig. S6). This suggests that peptides displaying similar scores for the two modes may preferentially adopt a bulged conformation.

Crystal structures of C-terminally extended HLA-I ligands

To investigate the structural mechanisms underlying C-terminal extensions uncovered in this work, we generated a high resolution (1.6Å) crystal structure of HLA-A68:01 in complex with a 10-mer peptide (ETSPLTAEKL, Fig. 3) predicted to follow the C-terminal extension binding mode (SI Appendix, Fig. 4A and SI Appendix, Fig. S7). As expected, the lysine at P9 (yellow sidechain) filled the F pocket and superimposed nicely with the last residue (K9) of canonical 9-mer ligands of HLA-A68:01 (blue sidechain in Fig. 4A). More importantly, in order to accommodate the C-terminal extension (L10), the Y84 sidechain was flipped by 90 degrees and the two alpha helices around the F pocket moved away from each other (Fig. 4A), as measured by the distance between C-alpha atoms of residues 80 and 143 ($D_{80-143}=11.1\text{\AA}$ versus $D_{80-143}=10.1\text{\AA}$ for the complex with a 9-mer peptide). Interestingly, the same flip had been observed in one of the HLA-A02:01 structures in complex with C-terminally extended ligands (9) (Fig. 4B). However, in contrast to HLA-A02:01 where the sidechain of the first residue of the C-terminal extension points towards the solvent (K12 Fig. 4B (9), see also L10 in PDB:5FA4 and D10 in PDB:5F7D (10)), in the case of HLA-A68:01, the C-terminal extension sidechain filled the pocket created by the flip of Y84 sidechain (SI Appendix, Fig. S8). This result is fully consistent with the specificity for hydrophobic residues in the C-terminal extension motif of HLA-A68:01 (Fig. 2A). It is also interesting to note that the flip of Y84 sidechain was recently observed in a crystal structure of peptide-MHC-β2m in complex with

TAPBPR, suggesting that loading of C-terminal extensions may be favored *in vivo* (20).

SI Appendix (Fig. S4) shows that the hydrophobic sidechain at P10 is not strictly required and peptides with S or D at this position can bind. In these cases, we anticipate that the P10 sidechain points towards the solvent, as in previous structures of HLA-A02:01 in complex with C-terminal extensions, although we cannot exclude that additional structural changes may further modify the physical properties of the new pocket to accommodate polar or charged amino acids.

Propensity of HLA-I alleles for C-terminal extensions

To investigate the molecular determinants of C-terminal extensions, we aligned the sequences of all HLA-I alleles considered in this work and checked whether some amino acid patterns in residues surrounding the F pocket characterize alleles predicted to accommodate C-terminal extensions (SI Appendix). Clear differences were observed at specific positions (Fig. 4C) and showed overlap with properties characterizing HLA-A alleles, as expected from the higher proportion of HLA-A alleles predicted to display C-terminal extensions (Fig. 2A). Interestingly, glycine is known to destabilize alpha helices and the presence of glycine at position 79 (i.e., exactly where the α_1 helices start to be no longer aligned in Fig. 4A) in most HLA-I alleles predicted to display C-terminal extensions may endow the α_1 helix with the flexibility required to accommodate such extensions. To test whether these amino acid patterns may help predict whether an allele is more likely to display C-terminal extensions, we trained a logistic regression and performed a rigorous cross-validation (SI Appendix). An average Area Under the ROC Curve (AUC) of 0.85 could be obtained, suggesting that alleles accommodating C-terminal extensions may be reasonably well predicted from their sequence. Lower accuracy was reached in a simple model where HLA-A alleles are predicted to display C-terminal extensions and HLA-B/C alleles are not (AUC=0.76). To further investigate molecular mechanisms allowing for C-terminal extensions, we surveyed available X-ray structures of HLA-I alleles considered in this work (SI Appendix, Table S1). As before, we computed the distance between the two alpha helices surrounding the C-terminus of canonical ligands (SI Appendix, Table S1). Interestingly, we observed that, on average, alleles predicted to display C-terminal extensions showed larger distances between these two helices already when

interacting with canonical 9-mer peptides ($P=0.002$, Wilcoxon rank-sum test, Fig. 4D). Using this distance to predict alleles accommodating C-terminal extensions among those with available crystal structures led to an AUC of 0.92. Of note, HLA-B51:01 is characterized by much higher frequency of 8-mer ligands compared to other HLA-I alleles (2, 3, 21). As for HLA-A01:01, we observed a trend for C-terminal extensions in some samples (e.g., the mono-allelic cell line), but not in other samples (e.g., Melanoma/Mel_12, see Dataset S2 and SI Appendix, Fig. S9, although most 10-mer peptides in this sample should come from HLA-A01:01 since HLA-B08:01 and HLA-C07:01 poorly bind 10-mers). We finally point out that the clear patterns in both sequence and structural properties of HLA-I alleles predicted to display C-terminal extensions provides an additional and independent validation of our predictions in Fig. 2 based only on HLA peptidomics data.

Explicitly incorporating C-terminal extensions in HLA-I ligand predictors

C-terminal extensions have not been routinely investigated in previous studies and the training set of most existing HLA-I ligand predictors typically does not include them, even if recent version of NetMHC tools can mathematically handle them (22, 23). We therefore retrained our predictor MixMHCpred (19) using multiple PWMs to model C-terminal extensions (24) (SI Appendix). To validate our new algorithm, we took advantage of the fact that HLA-A03:01 and HLA-A68:01 alleles were present in multiple datasets and attempted to re-predict all the 10-mer peptides of these datasets, excluding data from the dataset used for testing in the training of our predictor (SI Appendix). As negative data, we included 4-fold decoy (i.e., 10-mers randomly selected from the human proteome) and computed both the Positive Predictive Value corresponding to the top 20% predictions and the AUC (SI Appendix). We observed that explicitly modeling C-terminal extensions increased the performance compared to the previous version of our predictor (MixMHCpred1.0) (19), as well as other widely used HLA-I ligand predictors that did not include unbiased MS data in their training set (22, 23) (Fig. 5A and SI Appendix, Fig. S10). The improvement came mainly from higher scores for ligands displaying C-terminal extensions, as shown in Fig. 5B for the HLA-A03:01 10-mer ligands isolated from a mono-allelic cell line (2) ($P=1.0 \times 10^{-7}$, Wilcoxon signed-rank test).

Almost no difference between MixMHCpred1.0 and MixMHCpred1.1 could be observed when testing our algorithm on other datasets used in previous benchmarking

studies. However, we anticipate that C-terminal extensions are very rare in these datasets since most of the known HLA-I ligands had been first predicted with former versions of HLA-I ligand predictors. For instance, when analyzing IEDB data (25) for HLA-A03:01 ligands coming from earlier studies than those considered in this work, we could not see any statistical evidence of C-terminal extensions, suggesting that such ligands had not been tested in binding assays, or had been filtered in MS data.

Identification of immunogenic C-terminally extended epitopes

To investigate the immunological relevance of HLA-I ligands displaying C-terminal extensions, we used our new predictor and scanned both human cancer testis antigens and viral proteomes with the motifs characterizing 10-mer C-terminal extensions for HLA-A03:01 and HLA-A68:01 (SI Appendix). This analysis revealed many putative epitopes, including peptides from the PRAME cancer testis antigen and several CMV, EBV, HIV, HPV, Influenza and Yellow Fever peptides (Table 1). We measured the binding stability of these peptides and found values falling within the range of CD8 T cell epitopes (Table 1).

We then focused on one CMV peptide binding to HLA-A03:01 (TVRSHCVSKI, star in Table 1). We stimulated a peripheral blood mononuclear cells (PBMCs) sample from a healthy donor (both HLA-A03:01 and CMV seropositive) with the 10-mer peptide for 12 days (Materials and Methods). Subsequently we observed cytokine production by IFN γ -ELISpot after re-challenge with the CMV 10-mer peptide for 16h (Fig. 5C), suggesting that this epitope is potentially immunogenic in human. To determine whether CD8 T cells could directly recognize the C-terminally extended 10-mer peptide, we constructed HLA-A03:01 tetramers loaded with the 10-mer peptide (Materials and Methods). Analyzing CD8 T cells with such tetramers revealed a population of CD8 T cells that directly bound to the C-terminally extended 10-mer peptide/HLA-A03:01 complex (Fig. 5D). The IFN γ -ELISpot, tetramer and refolding assays were repeated using the K(9)L and I(10)L mutants, and the 9-mer (SI Appendix, Fig. S11A-C). In all cases we could detect IFN γ production after stimulation (SI Appendix, Fig. S11A). Tetramer analysis revealed that T cells directly interacting with each of these epitopes could be identified, although the responses were not very strong (SI Appendix, Fig. S11B). The 9-mer displayed the strongest binding stability which, together with the preference of K/R of HLA-A03:01 at the

second anchor position, suggests that the 10-mer CMV epitope follows the predicted C-terminal extension binding mode (SI Appendix, Fig. S11C). However, we also observed residual binding of the K(9)L mutant (similar to what was observed in Fig. 3 for the first P9 mutant). To provide further evidences that the 10-mer CMV epitope follows the C-terminal extension binding mode, we tested the cross-reactivity of T cells with the 10- and 9-mer peptides (SI Appendix). We observed that T cells recognizing the 10-mer peptide were all cross-reactive with the 9-mer peptide (SI Appendix, Fig. S11D). This level of cross-reactivity is expected with C-terminal extensions since residues in contact with the TCR are structurally conserved, but is not expected with bulging 10-mers. Altogether these results suggests that TVRSHCVSKI follows the predicted C-terminal extension binding mode, and that C-terminally extended peptides can form *bona fide* CD8 T cell epitopes.

Discussion

MS analysis provides an unbiased view of HLA-I ligands that is not restricted by *a priori* assumptions on HLA-I binding specificity. Here we capitalized on this premise to explore non-canonical binding modes of HLA-I ligands. Out of the 54 alleles considered in this work, we found clear statistical evidences of C-terminal extensions for eight of them and validated these predictions at the biochemical and structural level for some of frequent alleles in Caucasian populations.

In addition to providing evidences of C-terminal extensions, our work enabled us to characterize new motifs describing this non-canonical binding mode. We observed that the C-terminal extensions are often characterized by the presence of hydrophobic residues. We also note that, for three out of eight alleles (i.e., HLA-A03:01, HLA-A31:01 and HLA-A68:01), a positively charged residue is found at the second anchor. This positively charged residue interacts with D77 and D116 in our HLA-A68:01 structure, which is consistent with the fact that D is preferentially observed at these positions in alleles predicted to accommodate C-terminal extensions (Fig. 4C). The distinct binding specificity between the anchor residue and the C-terminal extension makes these cases especially amenable for the sequence based model that we developed. However, the majority of alleles show preference for hydrophobic residues at the last position. In these cases, and assuming that the preference for hydrophobic residues at the C-terminal extension is conserved, sequenced-based

algorithms cannot unambiguously determine whether a 10-mer peptide with 2 hydrophobic amino acids at the last two positions follows the bulge or the C-terminal extension binding mode. Moreover, we anticipate that competition with high affinity 9-mer ligands may mask cases of lower affinity C-terminal extensions in HLA peptidomics data (e.g., peptides with only one good anchor residue). Therefore our estimate of the number of alleles that accommodate C-terminal extensions corresponds to a lower bound and we cannot exclude that this non-canonical binding mode may be observed in other alleles. In particular, some C-terminal extensions among HLA-A02:01 ligands may be present in our data with two hydrophobic residues at the last positions. Nevertheless, the smaller distance between the two alpha helices of HLA-A02:01 (Fig. 4D) suggests that C-terminal extensions for this allele should be rarer, or involve other mechanisms like cross-presentation (9, 10). Along this line, we note that statistically significant C-terminal extensions are identified by our algorithm in the set of *T. gondii* HLA-A02:01 ligands (9) (SI Appendix, Table S2).

Finally, we stress that contaminations from co-eluting or wrongly identified peptides, as well as challenges in aligning small peptides or in the deconvolution of pooled HLA peptidomics datasets, can easily result in cases that look like N- or C-terminal extensions. This is the reason why we developed the statistical framework described in this work and tested the robustness of our predictions with respect to noise.

Despite these inherent limitations of sequence-based approaches, it is likely that several alleles show very few, if any C-terminal extensions. For instance, six alleles from our list showed specificity at the last anchor residue that is not restricted to hydrophobic amino acids (SI Appendix, Fig. S12) but we did not see any trend of C-terminal extensions among their 10-mer ligands (Dataset S2).

Our model also incorporated the possibility to have N-terminal extensions but we did not find any such event, although N-terminal extensions have been recently reported (11, 12). Inspection of existing structures of HLA-I molecules in complex with 9-mer peptides shows that the C-terminal carboxyl group of 9-mer HLA-I ligands is often partly solvent exposed. Conversely, the N-terminal amide group points in general towards the binding site. This likely explains why N-terminal extensions appear to be much less frequent, although we cannot exclude that our approach may miss some N-terminal extensions if the specificity at P2 is the same as at P3 in the N-terminally extended ligands. Interestingly, this appears to be the case for N-terminal extensions

reported for HLA-B57:01 and may explain why these extensions could not be easily detected with sequence-based approaches and have been first identified by X-ray crystallography (11).

Our demonstration of direct recognition by human CD8 T cells of a peptide predicted to follow the C-terminal extension binding mode indicates that these extensions are compatible with TCR binding. This did not come as a surprise since amino acids in contact with the TCR (typically position 4 to 7) are structurally conserved between 9-mers and C-terminally extended 10-mers, which is consistent with the cross-reactivity observed in SI Appendix, Fig. S11D. Moreover, the vast repertoire of TCR enables recognition of many different types of epitopes (e.g., bulges, post-translational modifications), so that the small changes in the positioning of the two alpha helices were not expected to prevent TCR recognition. C-terminal extensions may further play a role in the binding of KIR proteins, which are known to recognize amino acids surrounding the C-terminus of canonical HLA-I ligands (11, 26, 27). Along these lines, we note that the HIV peptides in Table 1 represent a known escape mutant (NEF A83G), which was previously proposed to act at the level antigen processing (28). Our results suggest that this mutation may also have an effect on recognition of peptide-HLA complexes by NK receptors. As such, we anticipate that inclusion of C-terminal extensions in the new version of our HLA-I ligands predictor may help uncovering new CD8 T cell epitopes in viruses or tumors, as well as potential targets of NK cells.

Overall, our results reveal frequent C-terminal extensions in at least eight out of the 54 HLA-I alleles analyzed in this study and highlight the power of unbiased HLA peptidomics data together with new algorithms to unravel novel properties of HLA-I molecules. Our evidence of direct T cell recognition of such epitopes suggests that C-terminal extensions may be clinically relevant for infectious diseases or cancer immunotherapy.

Materials and Methods

Binding stability measurements were performed with standard refolding assays and stable complexes were detected with ELISA. X-ray crystallography was carried out as described in SI Appendix. The model and structure factors have been deposited with PDB accession code 6EI2. PBMCs were peptide stimulated in vitro for 12 days in

vitro in presence of 100 U/ml IL-2. Subsequently, the Elispot was performed using the ELISpot^{PRO} kit for Human IFN γ from MABTECH. CD8 T cells of the CMV 10-mer peptide stimulated PBMC were stained with a PE labeled HLA-A03:01/TVRSHCVSKI multimer and co-stained with anti-CD8 antibody (BC A94683). Multimer+ CD8+ T cells were analysed at the BD ARIA III instrument equipped with the FACS Diva software.

The code for identifying C- and N-terminal extensions (MHCpExt) and the new version of the predictor (MixMHCpred1.1) are available at <https://github.com/GfellerLab> and algorithmic details about the new methods are available in SI Appendix.

Acknowledgment

We thank Julien Racle and Santiago Carmona for a critical reading of the manuscript. We thank Anne Wilson and her collaborators of the flow cytometry facility, and the members of our laboratories for their support. D.G. acknowledges the financial support of CADMOS. S.P. and P.F. acknowledge support from SGC, a registered charity (number 1097737) that receives funds from AbbVie, Bayer Pharma AG, Boehringer Ingelheim, Canada Foundation for Innovation, Eshelman Institute for Innovation, Genome Canada, Innovative Medicines Initiative (EU/EFPIA) (ULTRA-DD Grant 115766), Janssen, Merck & Co., Novartis Pharma AG, Ontario Ministry of Economic Development and Innovation, Pfizer, Sao Paulo Research Foundation-FAPESP, Takeda, and the Wellcome Trust (092809/Z/10/Z). P.F., and S.P. are supported by a Wellcome Career Development Fellowship (095751/Z/11/Z). We also thank Diamond Light Source for access to beamline I24 (proposal number mx15433). Computations were performed at the Vital-IT (<http://www.vital-it.ch>) Center for high-performance computing of the Swiss Institute of Bioinformatics.

References

1. Trolle T, et al. (2016) The Length Distribution of Class I-Restricted T Cell Epitopes Is Determined by Both Peptide Supply and MHC Allele-Specific Binding Preference. *J Immunol* 196(4):1480–1487.

2. Abelin JG, et al. (2017) Mass Spectrometry Profiling of HLA-Associated Peptidomes in Mono-allelic Cells Enables More Accurate Epitope Prediction. *Immunity* 46(2):315–326.
3. Andreatta M, Alvarez B, Nielsen M (2017) GibbsCluster: unsupervised clustering and alignment of peptide sequences. *Nucleic Acids Res* 45(W1):W458–W463.
4. Bassani-Sternberg M, Gfeller D (2016) Unsupervised HLA Peptidome Deconvolution Improves Ligand Prediction Accuracy and Predicts Cooperative Effects in Peptide-HLA Interactions. *J Immunol* 197(6):2492–2499.
5. Jurtz V, et al. (2017) NetMHCpan-4.0: Improved Peptide-MHC Class I Interaction Predictions Integrating Eluted Ligand and Peptide Binding Affinity Data. *J Immunol* 199(9):3360–3368.
6. Guo HC, et al. (1992) Different length peptides bind to HLA-Aw68 similarly at their ends but bulge out in the middle. *Nature* 360(6402):364–366.
7. Collins EJ, Garboczi DN, Wiley DC (1994) Three-dimensional structure of a peptide extending from one end of a class I MHC binding site. *Nature* 371(6498):626–629.
8. Tenzer S, et al. (2009) Antigen processing influences HIV-specific cytotoxic T lymphocyte immunodominance. *Nat Immunol* 10(6):636–646.
9. McMurtrey C, et al. (2016) Toxoplasma gondii peptide ligands open the gate of the HLA class I binding groove. *Elife* 5:246.
10. Remesh SG, et al. (2017) Breaking confinement: unconventional peptide presentation by major histocompatibility (MHC) class I allele HLA-A*02:01. *J Biol Chem* 292(13):5262–5270.
11. Pymm P, et al. (2017) MHC-I peptides get out of the groove and enable a novel mechanism of HIV-1 escape. *Nat Struct Mol Biol* 219:277.
12. Li X, Lamothe PA, Walker BD, Wang J-H (2017) Crystal structure of HLA-B*5801 with a TW10 HIV Gag epitope reveals a novel mode of peptide presentation. *Cell Mol Immunol* 14(7):631–634.
13. Stryhn A, Pedersen LO, Holm A, Buus S (2000) Longer peptide can be accommodated in the MHC class I binding site by a protrusion mechanism. *Eur J Immunol* 30(11):3089–3099.
14. Bassani-Sternberg M, et al. (2016) Direct identification of clinically relevant neoepitopes presented on native human melanoma tissue by mass spectrometry. *Nat Commun* 7:13404.
15. Bassani-Sternberg M, Pletscher-Frankild S, Jensen LJ, Mann M (2015) Mass spectrometry of human leukocyte antigen class I peptidomes reveals strong effects of protein abundance and turnover on antigen presentation. *Mol Cell Proteomics* 14(3):658–673.

16. Ritz D, et al. (2016) High-sensitivity HLA class I peptidome analysis enables a precise definition of peptide motifs and the identification of peptides from cell lines and patients' sera. *Proteomics* 16:1570–1580.
17. Mommen GPM, et al. (2014) Expanding the detectable HLA peptide repertoire using electron-transfer/higher-energy collision dissociation (ET_hCD). *Proc Natl Acad Sci USA* 111(12):4507–4512.
18. Hilton HG, et al. (2017) The Intergenic Recombinant HLA-B*46:01 Has a Distinctive Peptidome that Includes KIR2DL3 Ligands. *Cell Rep* 19(7):1394–1405.
19. Bassani-Sternberg M, et al. (2017) Deciphering HLA-I motifs across HLA peptidomes improves neo-antigen predictions and identifies allosteric regulating HLA specificity. *PLoS Comput Biol* 13(8):e1005725.
20. Jiang J, et al. (2017) Crystal structure of a TAPBPR-MHC I complex reveals the mechanism of peptide editing in antigen presentation. *Science* 358(6366):1064–1068.
21. Guasp P, et al. (2016) The Peptidome of Behçet's Disease-Associated HLA-B*51:01 Includes Two Subpeptidomes Differentially Shaped by Endoplasmic Reticulum Aminopeptidase 1. *Arthritis Rheumatol* 68(2):505–515.
22. Nielsen M, Andreatta M (2016) NetMHCpan-3.0; improved prediction of binding to MHC class I molecules integrating information from multiple receptor and peptide length datasets. *Genome Med* 8(1):33.
23. Andreatta M, Nielsen M (2016) Gapped sequence alignment using artificial neural networks: application to the MHC class I system. *Bioinformatics* 32(4):511–517.
24. Gfeller D, et al. (2011) The multiple-specificity landscape of modular peptide recognition domains. *Mol Syst Biol* 7(1):484–484.
25. Vita R, et al. (2015) The immune epitope database (IEDB) 3.0. *Nucleic Acids Res* 43(Database issue):D405–12.
26. Malnati MS, et al. (1995) Peptide specificity in the recognition of MHC class I by natural killer cell clones. *Science* 267(5200):1016–1018.
27. Vivian JP, et al. (2011) Killer cell immunoglobulin-like receptor 3DL1-mediated recognition of human leukocyte antigen B. *Nature* 479(7373):401–405.
28. Chassin D, et al. (1999) Dendritic cells transfected with the nef genes of HIV-1 primary isolates specifically activate cytotoxic T lymphocytes from seropositive subjects. *Eur J Immunol* 29(1):196–202.
29. Niu L, et al. (2013) Structural basis for the differential classification of HLA-A*6802 and HLA-A*6801 into the A2 and A3 supertypes. *Mol Immunol* 55(3-4):381–392.

Figure Legend

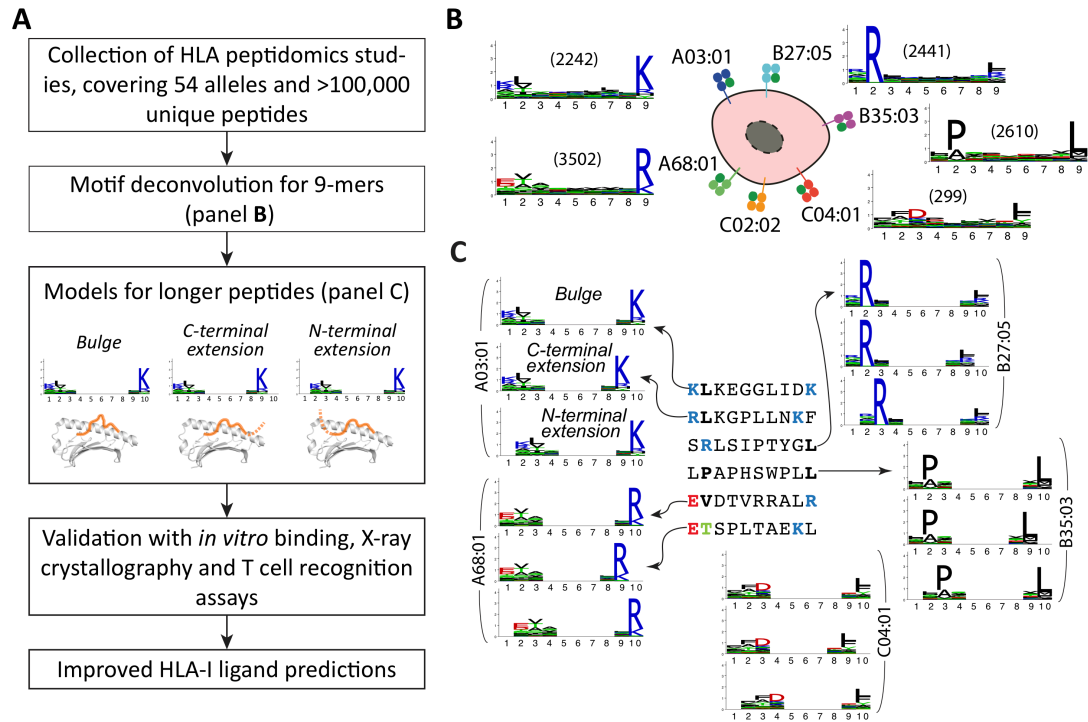


Fig. 1. A: General description of the pipeline developed in this work to identify and validate N- or C-terminal extensions. **B:** Example of 9-mer motifs identified in HLA peptidomics data from Mel_15 (14). The number of peptides assigned to each motif is shown in parentheses. **C:** Illustration of the different models built from the 9-mer motifs (bulge, C- and N-terminal extension) to investigate non-canonical binding modes among 10-mers.

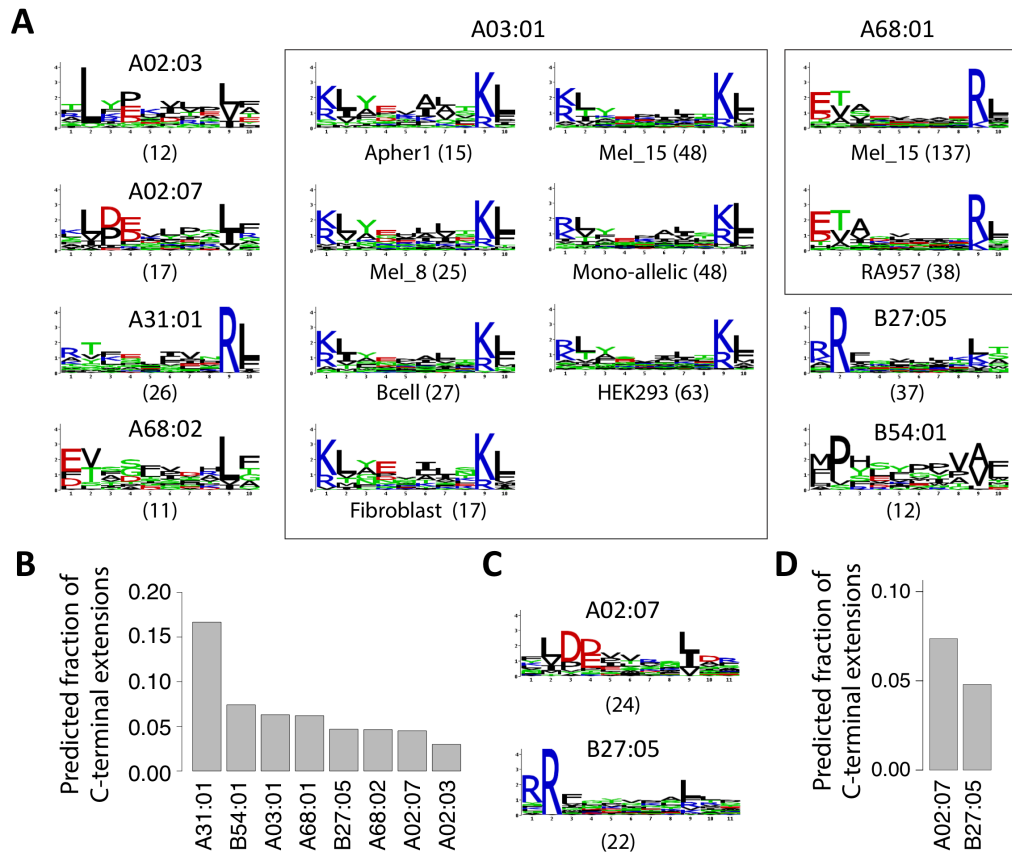


Fig. 2. A: Predicted 10-mer C-terminal extension motifs found for different HLA-I alleles in the different datasets (see also Datasets S2 and S3). Parentheses indicate the number of peptides associated to each motif. **B:** Estimates of the frequency of C-terminal extensions among 10-mers for alleles shown in A. **C:** C-terminal extensions motifs comprising two residues after the second anchor residue in 11-mers ligands. **D:** Estimates of the frequency of C-terminal extensions among 11-mers for alleles shown in C.

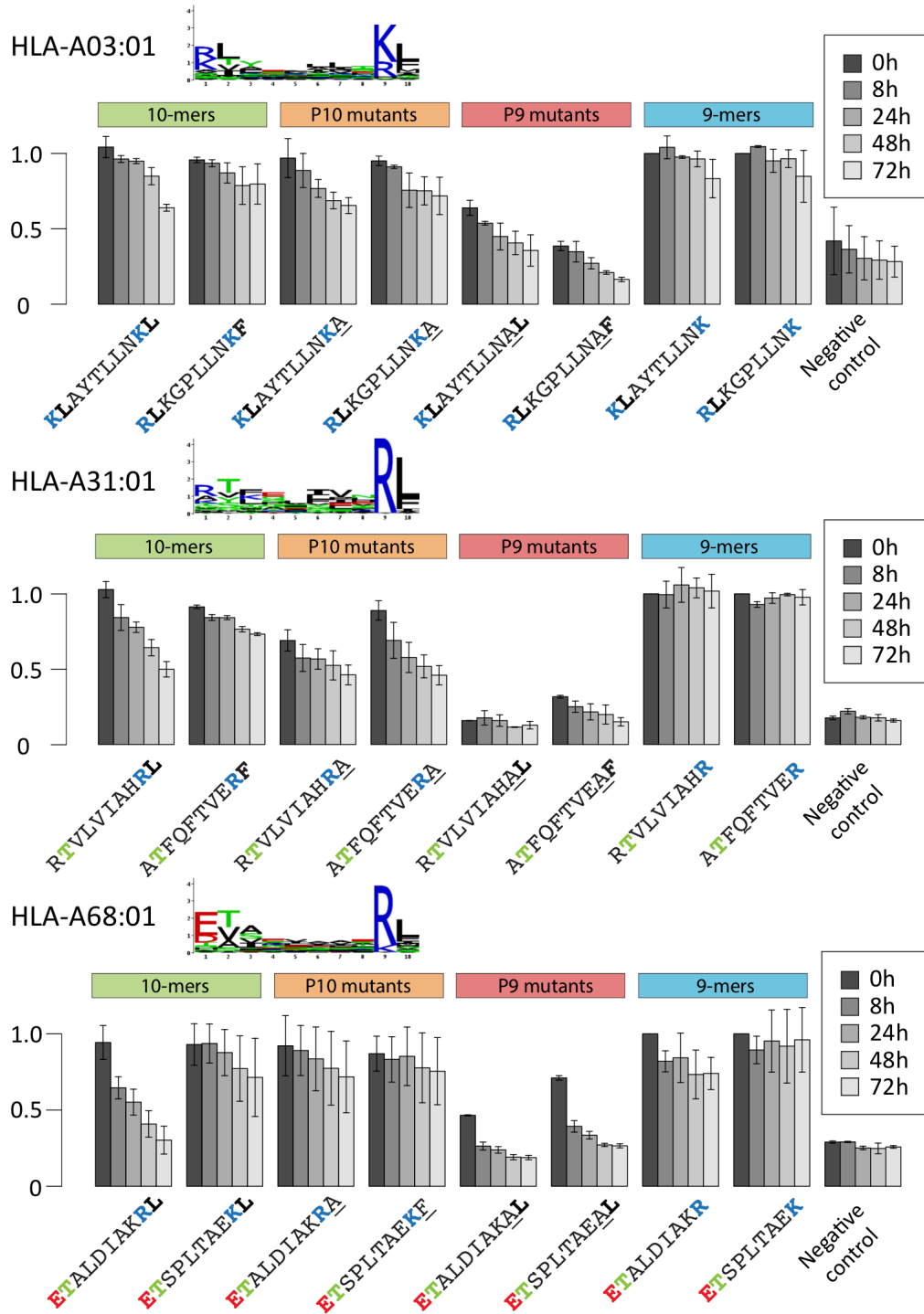


Fig. 3. In vitro binding stability assays for peptides predicted to follow the C-terminal extension binding mode for HLA-A03:01, HLA-A31:01, HLA-A68:01.

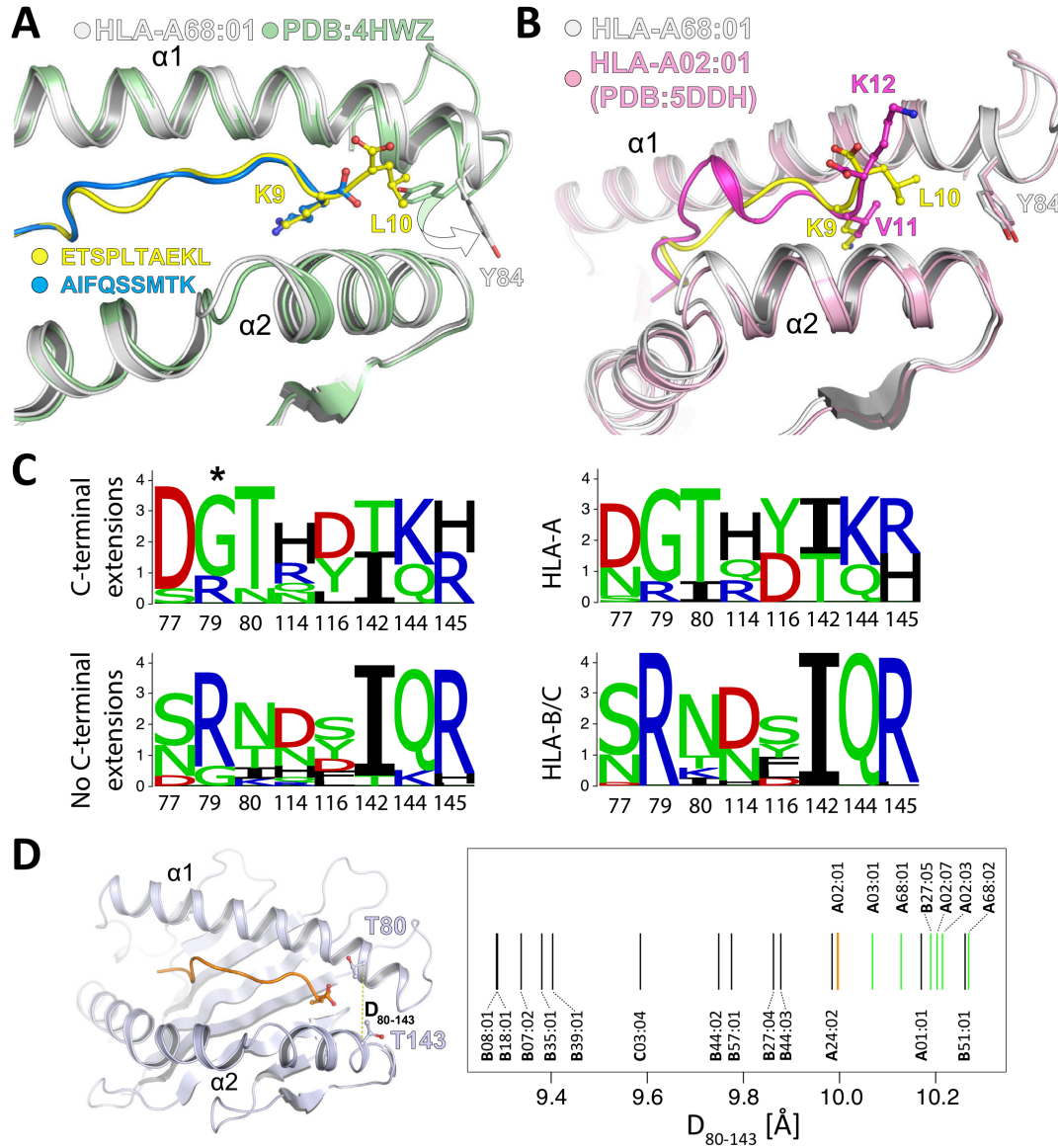


Fig. 4. A: New crystal structure of HLA-A68:01 (white ribbon) in complex with a C-terminally extended ligand (yellow) superimposed with HLA-A68:01 (green ribbon) in complex with a canonical 9-mer ligand (blue, PDB:4WHZ) (29). **B:** Comparison of HLA-A68:01 (white ribbon) in complex with a C-terminally extended ligand (yellow) and the complex of HLA-A02:01 (pink ribbon) bound to a C-terminal extended 12-mer peptide (FVLELEPEWTVK, magenta, PDB:5DDH) (9). **C:** HLA-I residues surrounding the C-terminus of canonical ligands and displaying the largest Jensen-Shannon divergence between alleles with C-terminal extensions (top left) and alleles without C-terminal extensions (bottom left). For comparison, the sequence logos of HLA-A (top right) and HLA-B/C (bottom right) alleles at the same positions are displayed. **D:** Analysis of the distance D_{80-143} for alleles with available crystal

structures (SI Appendix, Table S1). Green lines correspond to alleles displaying C-terminal extensions. The orange line represents HLA-A02:01.

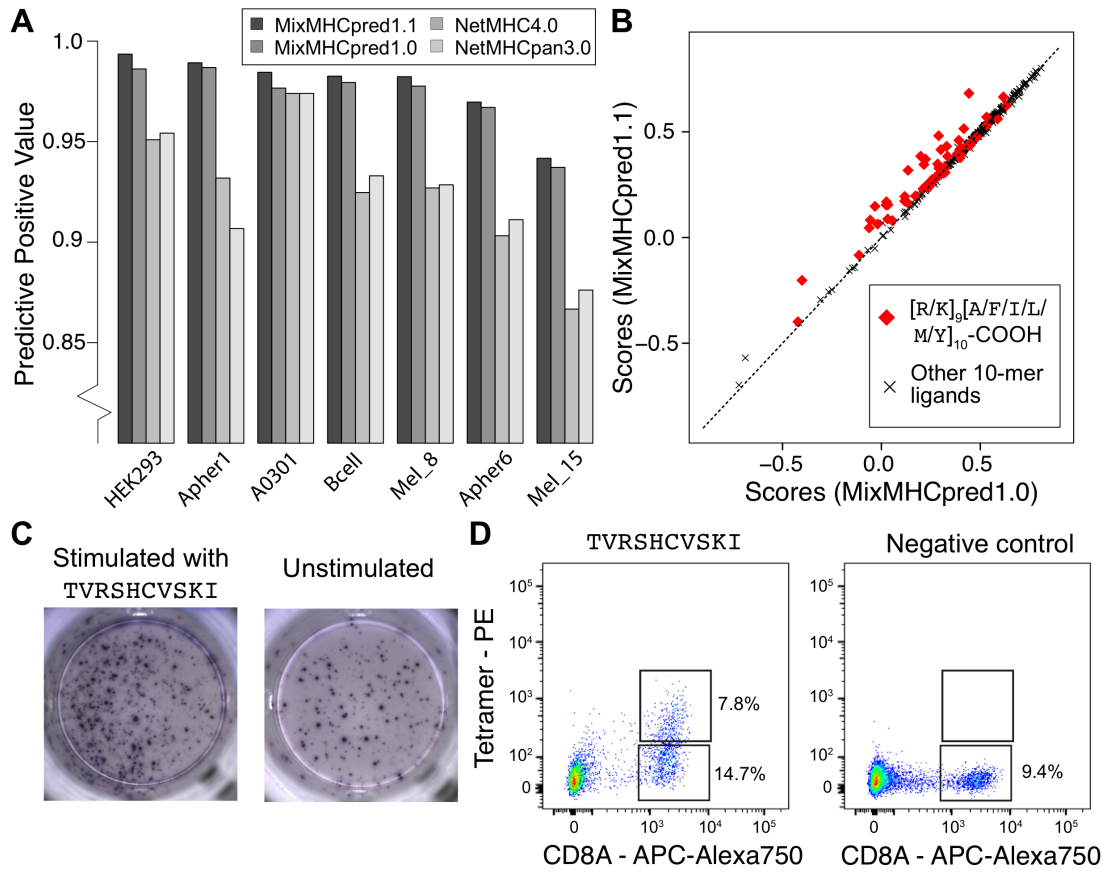


Fig. 5. A: Benchmarking of the new version of our HLA-I ligand predictor (MixMHCpred1.1). The y-axis shows the Positive Predictive Value among the top 20% of the predictions. **B:** Analysis of scores when explicitly modeling C-terminal extensions (MixMHCpred1.1) or not (MixMHCpred1.0) for the 10-mer HLA-A03:01 ligands from a mono-allelic cell line (2), as a function of the C-terminal amino acids (P9 and P10). **C:** IFN γ -ELISpot results obtained by stimulation with a C-terminally extended 10-mer HLA-A03:01 ligand (TVRSHCVSKI, from CMV, left) vs. no peptide (right) of a PBMC sample from a HLA-A03:01 and CMV seropositive healthy donor. **D:** Multimer analysis of CD8 T cells from a healthy donor recognizing the HLA-A03:01 restricted C-terminally extended 10-mer peptide TVRSHCVSKI (left) and the negative control (RVRAYFYSKV/HLA-A03:01 tetramer) for which we did not observe T cell recognition (right).

Supporting Appendix

The C-terminal extension landscape of naturally presented HLA-I ligands

Running title: C-terminal extensions in HLA-I ligands.

Philippe Guillaume^a, Sarah Picaud^{b,c}, Petra Baumgaertner^a, Nicole Montandon^a, Julien Schmidt^a, Daniel E Speiser^a, George Coukos^a, Michal Bassani-Sternberg^a, Panagis Filippakopoulos^{b,c}, David Gfeller^{a,d,1,2}

^aLudwig Institute for Cancer Research, Department of Fundamental Oncology, University of Lausanne, 1066 Epalinges, Switzerland.

^bStructural Genomics Consortium, Old Road Campus Research Building, Roosevelt Drive, Nuffield Department of Clinical Medicine, University of Oxford, Roosevelt Drive, Oxford OX3 7DQ, UK.

^cLudwig Institute for Cancer Research, Nuffield Department of Clinical Medicine, University of Oxford, Roosevelt Drive, Oxford OX3 7DQ, UK.

^dSwiss Institute of Bioinformatics (SIB), 1015 Lausanne, Switzerland.

¹ To whom correspondence should be sent: David.Gfeller@unil.ch.

² D.G. should be considered both as first and last author.

SI Methods

Collection of HLA peptidomics data

HLA peptidomics data used in this study came from seven different studies (1-7) (Dataset S1). In all these studies, peptides were eluted from class I specific antibody purified HLA molecules. None of these data had been filtered with existing predictors, and therefore all had the potential to reveal non-canonical ligands. We only included MS samples generated with $< 1\%$ false discovery rate, with available HLA-I typing information and in which HLA-I motifs could be clearly annotated by our motif deconvolution approach for pooled HLA peptidomics data (7, 8). In total, our dataset comprises 43 samples covering 54 different HLA-I alleles (Dataset S1) for a total of 109,953 unique peptides (9- to 12-mers).

Analysis of non-canonical binding modes

Analysis of 9-mer HLA peptidomes

To analyze non-canonical binding modes in pooled HLA peptidomics studies that include ligands from up to six different HLA-I molecules, we developed the pipeline illustrated in Fig. 1. We first characterized the different motifs of the 9-mer HLA peptidomes using our recent motif deconvolution algorithm (8) (Fig. 1B). This algorithm has the major advantage of not depending on *a priori* knowledge of HLA-I binding specificity, and therefore can be applied even in the presence of poorly characterized HLA-I alleles. Each 9-mer peptide was then assigned to its corresponding motif and PWMs were built for each group of peptides, including random counts based on BLOSUM62 (7).

Prediction of N- and C-terminal extensions

To distinguish between the three different models describing longer peptides (i.e. bulge, N-terminal extensions, C-terminal extensions), we developed the algorithm illustrated in Fig. 1C. We first reasoned that longer peptides following the bulge model should have conserved binding specificity around the anchor residues at the second and last positions. We therefore modeled these peptides with the binding specificity of 9-mers at the first three and last two amino acids, and unspecific position in the middle. In the absence of *a priori* information about the amino acid

preferences at terminal extensions, we modeled them as with one unspecific position at the N- or C-terminus. To enable meaningful comparison between the scores of the bulge and the terminal extension models, we did not impose any constrain at middle positions in the N- or C-terminal extension models. Each longer peptide (i.e., L -mer, with L equal to 10, 11 or 12) was then scored with all models (i.e. bulge, N- or C-terminal extensions) derived from each motif identified in the 9-mer HLA peptidome. Scores for the different models were computed as:

$$\sum_{i=1}^3 \log \left(\frac{M_{X_i,i}}{P(X_i)} \right) + \sum_{i=8}^9 \log \left(\frac{M_{X_{i+S},i}}{P(X_{i+S})} \right) \quad \text{for the bulge model;}$$

$$\sum_{i=1}^3 \log \left(\frac{M_{X_i,i}}{P(X_i)} \right) + \sum_{i=8}^9 \log \left(\frac{M_{X_i,i}}{P(X_i)} \right) \quad \text{for the C-terminal extension model and}$$

$$\sum_{i=1}^3 \log \left(\frac{M_{X_{i+S},i}}{P(X_{i+S})} \right) + \sum_{i=8}^9 \log \left(\frac{M_{X_{i+S},i}}{P(X_{i+S})} \right) \quad \text{for the N-terminal extension model,}$$

where M stands for the 20x9 PWM derived from 9-mer ligands for a given allele, X stands for the sequence of a L -mer peptide, S equals to $L-9$, and $P(X_i)$ stands for the frequency of amino acid X_i in the human proteome. Peptides were then assigned to one model and one allele if their score with this allele and this model was higher than a threshold T_1 and no other score for all the other possible models of any allele was larger than the largest score minus T_2 . Here we chose values of T_1 and T_2 equal to 2.0, since over 95% of the longer peptides found in our HLA peptidomics datasets had a score larger than this value for at least one allele and one model. We further developed a null model to assign Z-scores to the number of predicted C-terminal extensions with respect the expected number considering only bulges. Alleles with anchor residues at positions 4 to 7 (i.e., HLA-B08:01, HLA-B14:01 and HLA-B14:02) were excluded, as they display non-conserved binding motifs between 9- and 10-mers and much less 10-mer ligands (8).

The fractions of C-terminal extensions shown in Fig. 2B and 2D were computed as the number of peptides unambiguously assigned to the C-terminal extension mode of a given allele, divided by the number of peptides assigned to any of the three models for the same allele. Sequence logos were generated with the LOLA software (<http://baderlab.org/Software/LOLA>).

Null model

To account for possible noise in MS data and focus on predictions that showed statistical significance, we developed a null model representing the expected HLA peptidome from the bulge model, and described here for the case of 10-mer ligands.

Starting with a list 100'000 10-mer peptides randomly selected from the human proteome, we selected those that passed the threshold T_1 for the bulge model of at least one motif. The list of peptides was further randomly filtered so as to have the same number of peptides assigned to each allele as in the actual 10-mers HLA peptidomics data. We then re-predicted these peptides using all three models for each motif (Fig. 1C). This enabled us to assess how many 10-mer peptides generated from the bulge model of each allele could by chance be assigned to the N- or C-terminal extensions of any allele when considering the three models. The simulations were repeated 100 times to derive a Z-score. Only alleles with at least 50 10-mer peptides assigned to them, at least 10 peptides assigned to the C- or N-terminal extension model and with a Z-score larger than 2 were included in our predictions. Similar predictions were obtained using values ranging between 1.5 and 2.5 for the threshold T_1 , or using a different threshold T_1 for each motif given by the score corresponding to the top 2% predictions in a large set of 100'000 10-mer peptides randomly selected from the human proteome (Table S3).

In vitro binding assays

All peptides used in Fig. 3 and 5, Fig S3, S4 and S11 and Table 1 were synthesized with free N and C-termini (1mg of each peptide, > 80% purity) at the Protein and Peptide Chemistry Facility of UNIL. Peptides were incubated separately with denaturated HLA alleles refolded by dilution in the presence of biotinylated beta-2 microglobulin proteins at temperature $T=4^{\circ}\text{C}$ for 48 hours. The solution was then incubated at 37°C . Samples were retrieved at time $t=0\text{h}$, 8h, 24h, 48h and $t=72\text{h}$. Stable complexes indicating interactions between HLA-I molecules and the peptides were detected by ELISA. Signals for 9-mer ligands at time $t=0\text{h}$ were used for renormalization, while negative controls consisted of absence of peptides. Half-lives (Table 1) were computed as $\ln(2)/k_{\text{off}}$, where k_{off} were determined by fitting exponential curves to the light intensity values obtained by ELISA, after removing the background signal (i.e., no peptides). Two independent replicates were performed for each measurement.

Expression and purification of HLA-A68:01 and $\beta 2\text{M}$

The heavy chain HLA-A68:01 and the light chain β 2M were purified from inclusion-bodies (9) with some small modifications. Briefly, recombinant expression plasmids were transformed into BL21 (DE3) (HLA-A68:01) or XA90 strain (β 2M) bacteria. The cells were grown overnight in LB (Luria-Bertani medium) twice concentrated supplemented with 50 $\mu\text{g ml}^{-1}$ kanamycin or 100 $\mu\text{g ml}^{-1}$ ampicillin respectively at 37 °C. One litre of pre-warmed LB was inoculated with 10 ml of the overnight culture and was incubated at 37 °C. At an $\text{OD}_{600\text{ nm}}$ of 0.6, expression was induced for 8 h at 37 °C with 1.0 mM isopropyl- β -D-thiogalactopyranoside (IPTG). Cells were then harvested by centrifugation (8700xg, 15 min, 4 °C, Beckman Coulter Avanti J-20 XP centrifuge), and then re-suspended in lysis buffer (10 mM TRIS-HCl, pH 8.0 at 20 °C complemented with 100 $\mu\text{g ml}^{-1}$ Lysozyme (Sigma Aldrich), 250 units of Benzonase (Novagen), 1 mM EDTA and 1:1000 (v/v) Protease Inhibitor Cocktail III (Calbiochem)). After 20 min of continuous rocking at 22 °C, cells were lysed 3 times at 4 °C using a Basic Z-Model Cell Disrupter (Constant Systems Ltd, UK). Inclusion-bodies were isolated by centrifugation (16000xg for 1 h at 4 °C, JA 25.50 rotor, on a Beckman Coulter Avanti J-20 XP centrifuge). The supernatant was decanted and the contaminated material was removed by scrapping the outer rings (viscous and dark coloured) leaving the more compact and lighter coloured inner ring (containing the protein of interest) intact. The pellet was then fully dispersed in 20 ml of washing buffer (10 mM TRIS-HCl, pH 8.0 at 20 °C) complemented with 1:1000 (v/v) Protease Inhibitor Cocktail III (Calbiochem) and centrifuged again for 10 min (16000xg at 4 °C, JA 25.50 rotor, on a Beckman Coulter Avanti J-20 XP centrifuge). The washing/scrapping steps were repeated 5 times (until the outer rings vanished). The pellet containing the recombinant protein was then dissolved in 20 ml of solubilisation buffer (100 mM TRIS-HCl, pH 8.0 at 20 °C, 8 M urea). Insoluble material was precipitated by centrifugation (16000xg for 1 h at 4 °C, JA 25.50 rotor, on a Beckman Coulter Avanti J-20 XP centrifuge). Solubilized HLA-A68:01 heavy chain was immediately flash frozen in liquid nitrogen and stored at -80 °C. The recombinant β 2M protein in urea was refolded by dialysis against 10 mM TRIS-HCl pH7.0 using SnakeSkin® Dialysis tubing (3.500 MWCO, Thermo Scientific) and purified by ion exchange on Hi-Trap Q HP (5 ml, GE Healthcare) column, with a linear gradient from 0 to 100 mM NaCl. Fractions containing pure β 2M were dialysed

overnight against water, concentrated with a 10 MWCO concentrator (Amicon® Ultra, MILLIPORE) to 2 mg ml⁻¹, flash frozen in liquid nitrogen and stored at -80 °C.

HLA:β2M:peptide complex assembly

The protein complex was reconstituted by dilution of the denatured HLA-A68:01 heavy chain (3 μM) and β2M (6 μM) in presence of the peptide ([H]-E-T-S-P-L-T-A-E-K-L-[OH], 10 μM) into 200 ml of refolding buffer (100 mM TRIS-HCl, pH 8.0 at 20 °C, 400 mM L-Arginine HCl (Sigma Aldrich), 2 mM EDTA, 5 mM reduced L-glutathione (Sigma Aldrich), 0.5 mM oxidized L-glutathione (Sigma Aldrich) and with 1:1000 (v/v) Protease Inhibitor Cocktail III (Calbiochem)). The refolding mixture was incubated at 10 °C during 36 h under constant stirring. Every 12 h another batch of the denatured HLA-A68:01 heavy chain (3 μM) was added to the mix. The 200 ml were then concentrated to 5 ml using a 3 MWCO concentrator (Amicon® Ultra, MILLIPORE). The concentrated protein mixture was further submitted to exclusion size chromatography (HiLoad™ 16/60 Superdex™ 75 prep grade, on Äkta Pure GE Healthcare) and each peak collected was submitted to SDS-PAGE gel and mass spectrometry (Agilent 6530 QTOF (Agilent Technologies Inc. - Palo Alto, CA)) to assess the simultaneous presence of the 3 components of the complex. Fractions of interest were then stored at 4°C until further use.

Crystallization

Prior to crystallization, the buffer of the protein complex was exchanged to 25 mM MES pH6.5 at 20 °C and 150 mM NaCl on a Superdex™ 200 Increase 10/300 GL column using an Äkta Pure system (GE Healthcare). The complex was then concentrated to 10.96 mg ml⁻¹ final using a 3 kDa MWCO concentrator (Amicon® Ultra, MILLIPORE). Aliquots of the complex were set up for crystallization using a mosquito® crystallization robot (TTP Labtech, Royston UK). Coarse screens were typically setup onto Greiner 3-well plates using three different drop ratios of precipitant to protein per condition (100+50 nl, 75+75 nl and 50+100 nl). Crystallization was carried out using the sitting drop vapor diffusion method at 4 °C. Crystals were grown by mixing 100 nl of the protein complex (10.96 mg/ml) with 50 nl of reservoir solution containing 0.1 M HEPES pH 7.5, 12 % PEG3350, 0.005 M CoCl₂, 0.005 M NiCl₂, 0.005 M CdCl₂ and 0.005 M MgCl₂. Diffraction quality crystals grew within a few days.

Data Collection and Structure Refinement

Crystals were cryo-protected using the well solution supplemented with additional ethylene glycol and were flash frozen in liquid nitrogen. Data were collected at Diamond beamline I24 on a Pilatus3 6M detector at a wavelength of 0.96864 Å. Indexing and integration was carried out using XDS (10) and scaling was performed with SCALA (11). Initial phases were calculated by molecular replacement with PHASER (12) using a model of HLA/β2M peptide complex (PDB:5T6X). Initial models were built by ARP/wARP (13) followed by manual building in COOT (14). Refinement was carried out in REFMAC5 (15). Thermal motions were analyzed using TLSMD (16) and hydrogen atoms were included in late refinement cycles. Data collection and refinement statistics can be found in Table S4. The model and structure factors have been deposited with PDB accession code: 6EI2.

HLA-I sequence and structure analysis

For all 54 alleles considered in this work, the sequence of the peptide binding domains were retrieved from IMGT database (17) and aligned with MUSCLE (18). To investigate the molecular determinants of C-terminal extensions, we selected all amino acids surrounding the F pocket (75-81, 84, 114-118, 142-147, following residue numbering in HLA-I structures). The eight positions displaying the largest changes in amino acid frequencies (Jensen-Shannon divergence larger than 0.1) are shown in Fig. 4C. Using 20-dimensional encoding for each amino acid, we trained a logistic regression model based on *glmnet* package in R (19). Four-fold cross-validation was performed and repeated 10 times for different random seeds to compute AUCs.

Available HLA-I crystal structures were then collected for alleles considered in this work. In total, 20 alleles among those with available HLA peptidomics data had experimental X-ray crystal structures. For each allele, a reference structure was selected by prioritizing complexes with 9-mer ligands and highest resolution (Table S1). In each structure, the distance between the C-alpha of residues 80 and 143 was computed (Fig. 4D and Table S1). The AUC of a predictor using as input feature this distance was 0.92, which is comparable to the AUC of the predictor based on HLA-I

sequences when considering only the 20 HLA-I alleles with available crystal structures (AUC=0.93, three-fold cross-validation).

HLA-I ligand predictors explicitly incorporating C-terminal extensions

For each allele displaying C-terminal extensions, we retrained our predictor based on HLA peptidomics data modeling C-terminal extensions as multiple motifs. In practice, all 10-mer ligands predicted to follow the C-terminal extension mode of each allele were treated separately and a PWM (M^C) was built with them (7). All other 10-mer ligands (non-C-terminal extensions) were used to build another PWM describing the bulge model (M^b). For alleles with C-terminal extensions, the score of a 10-mer peptide $X=(X_1, \dots X_{10})$ with this predictor is then computed as:

$$S(X) = \frac{1}{10} \log \left\{ w^C \prod_{i=1}^{10} \frac{M_{X_i,i}^C}{P(X_i)} + w^b \prod_{i=1}^{10} \frac{M_{X_i,i}^b}{P(X_i)} \right\}$$

where w^C , respectively w^b , stands for the fraction of ligands predicted to follow C-terminal extensions, respectively bulges. For alleles without C-terminal extensions, the predictions did not change compared to the previous version of our predictor (7).

Benchmarking of the algorithm was done using HLA-A03:01 and/or HLA-A68:01 positive samples, since these are the two HLA-I alleles displaying C-terminal extensions in multiple samples in our collection of HLA peptidomics studies. Careful cross-validation was performed, where for each sample used as testing set, the predictor was trained only on the data from the other samples. To this end, we further excluded from our analysis samples where some other HLA-I alleles did not appear in other samples (i.e., Fibroblast and RA957). For each sample, 4-fold excess of random peptides from the human proteome were added as negatives and all peptides were ranked with our new predictor, using for each peptide the highest score across the different HLA-I alleles present in the sample. The fraction of positives found in the top 20% of the predictions (which in this case is equivalent to the recall since the number of true positives is equal to the number of predictions) as well as the AUC were then computed (Fig. 5A and Fig. S10). The performance of the predictor explicitly modeling C-terminal extensions (MixMHCpred1.1) was compared with the former version of MixMHCpred (v1.0, based on a single PWM for each allele) (7), NetMHC4.0 (20) and NetMHCpan3.0 (21).

Human PBMC, IFN γ -ELISpot assays and Multimer analysis

Healthy volunteers donated circulating leukocytes according to the standards of the Blood Transfusion Center in Epalinges, Switzerland (Service Vaudois de Transfusion Sanguine). Samples from patients were obtained under written informed consent following study protocol approval by the Human Research Ethics Committee of the Canton de Vaud (Switzerland).

PBMCs were peptide stimulated in vitro for 12 days in vitro in presence of 100 U/ml IL-2. Subsequently, the Elispot was performed using the ELISpot^{PRO} kit for Human IFN γ from MABTECH (3420-2APT-10), following the standard supplier instructions. 100'000 cells per well were re-challenged with the peptide for 16h. The spots were analysed by the iSpot Robot ELISpot reader (AutoImmun Diagnostika GMBH).

Monomeric HLA-A03:01/TVRSHCVSKI complexes were prepared by refolding procedures using heavy chain HLA-A03:01 and the light chain β 2M, as described before. The heavy chain contained added BSP (BirA enzyme Substrate Peptide). The enzymatic biotinylation of HLA-A3:01-BSP was performed over night at 25°C with ATP, biotin and the biotin ligase Bir A. Multimer complexes were prepared by mixing biotinylated HLA-A03:01/TVRSHCVSKI monomers with PE-labeled streptavidin (Invitrogen).

CD8 T cells of the CMV 10-mer peptide stimulated PBMC after 12 days in vitro stimulation were stained with a PE labeled HLA-A03:01/TVRSHCVSKI multimer and co-stained with anti-CD8 antibody (BC A94683) and DAPI for dead cell exclusion. Multimer+ CD8+ T cells were analysed at the BD ARIA III instrument equipped with the FACS Diva software. The analysis was performed with the FlowJo software (FLOWJO.LLC). The negative control consists of an EBV-derived peptides (RVRAYFYSKV)/HLA-A03:01 tetramer and a PBMC sample from another HLA-A03:01 and EBV seropositive healthy donor, for which we did not observe any recognition by CD8 T cells.

IFN γ -ELISpot, tetramer and refolding assays for the I(10)L, K(9)L and truncated 9-mer peptides derived from the CMV epitope were later carried out in the same way (Fig. S11A-C), including also the 10-mer CMV epitope as a positive control for the tetramer analysis. T cells recognizing the wild-type peptide (upper box in Fig. 5D) were further sorted, expanded and tested for cross-reactivity with the 9-mer epitope (Fig S11D).

SI Figures

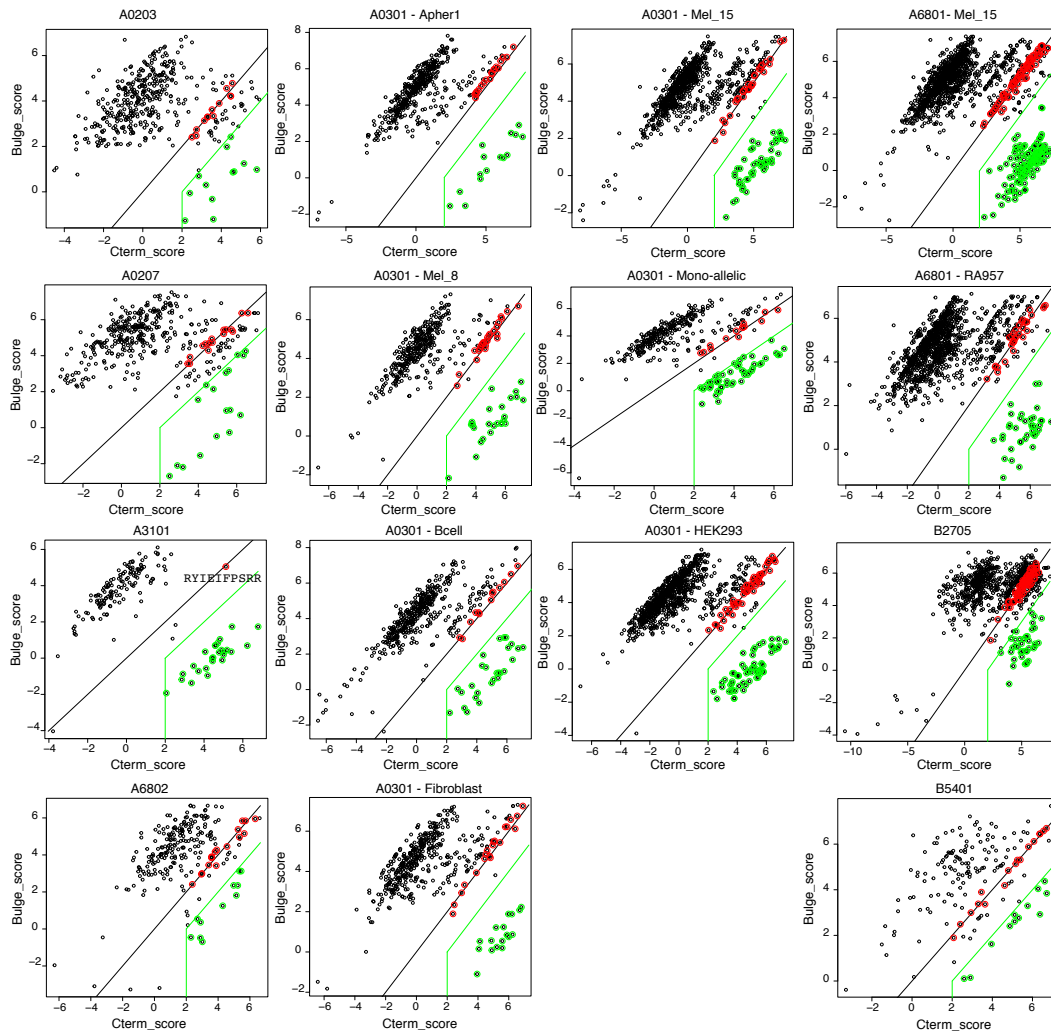


Fig. S1: Plots of the scores of peptides with the C-terminal extension model (x-axis) and the bulge model (y-axis) for all cases of predicted C-terminal extensions. Black lines show the $y=x$ line, green circles show predicted C-terminal extensions (Dataset S3), green lines represent the thresholds used (SI methods) and red circles show peptides with very similar scores with both models (Dataset S4). Only peptides unambiguously assigned to the corresponding allele in pooled samples are shown (SI Methods).

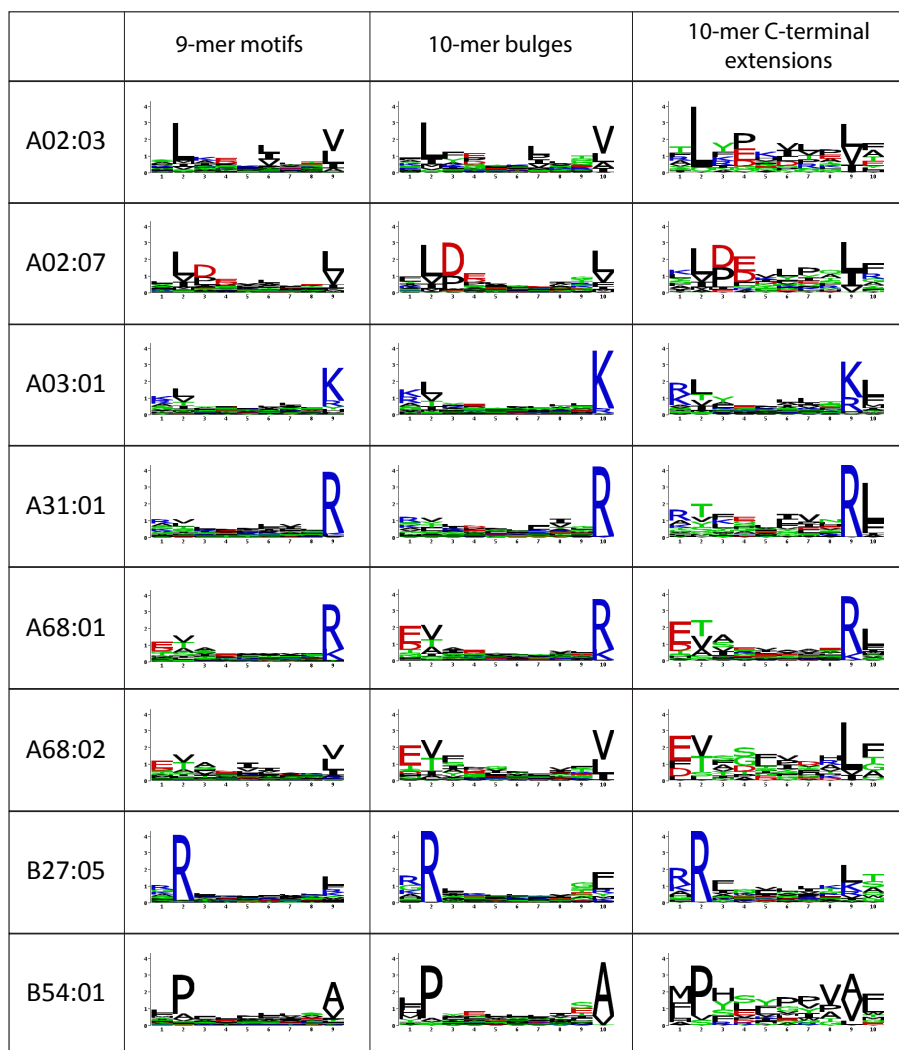


Fig. S2: Comparison between 9-mer motifs, 10-mer motifs from peptides predicted to follow the bulge model and 10-mer motifs from peptides predicted to display C-terminal extensions for the eight alleles with such extensions. For HLA-A03:01 and HLA-A68:01, peptides have been pooled from the different studies where C-terminal extensions were identified to generate the logos.

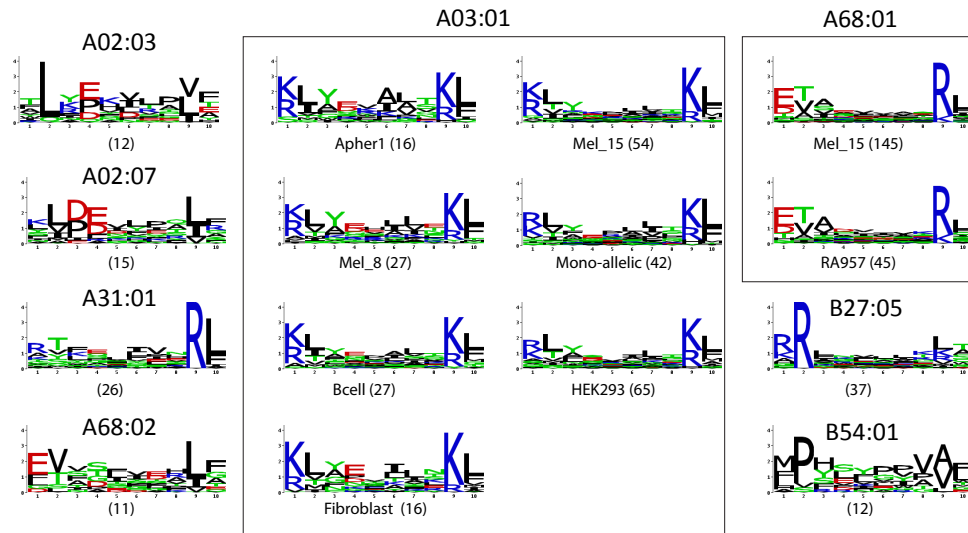


Fig. S3: Predictions of C-terminal extensions among 10-mer peptides in the presence of 5% of noise in all HLA peptidomics datasets.

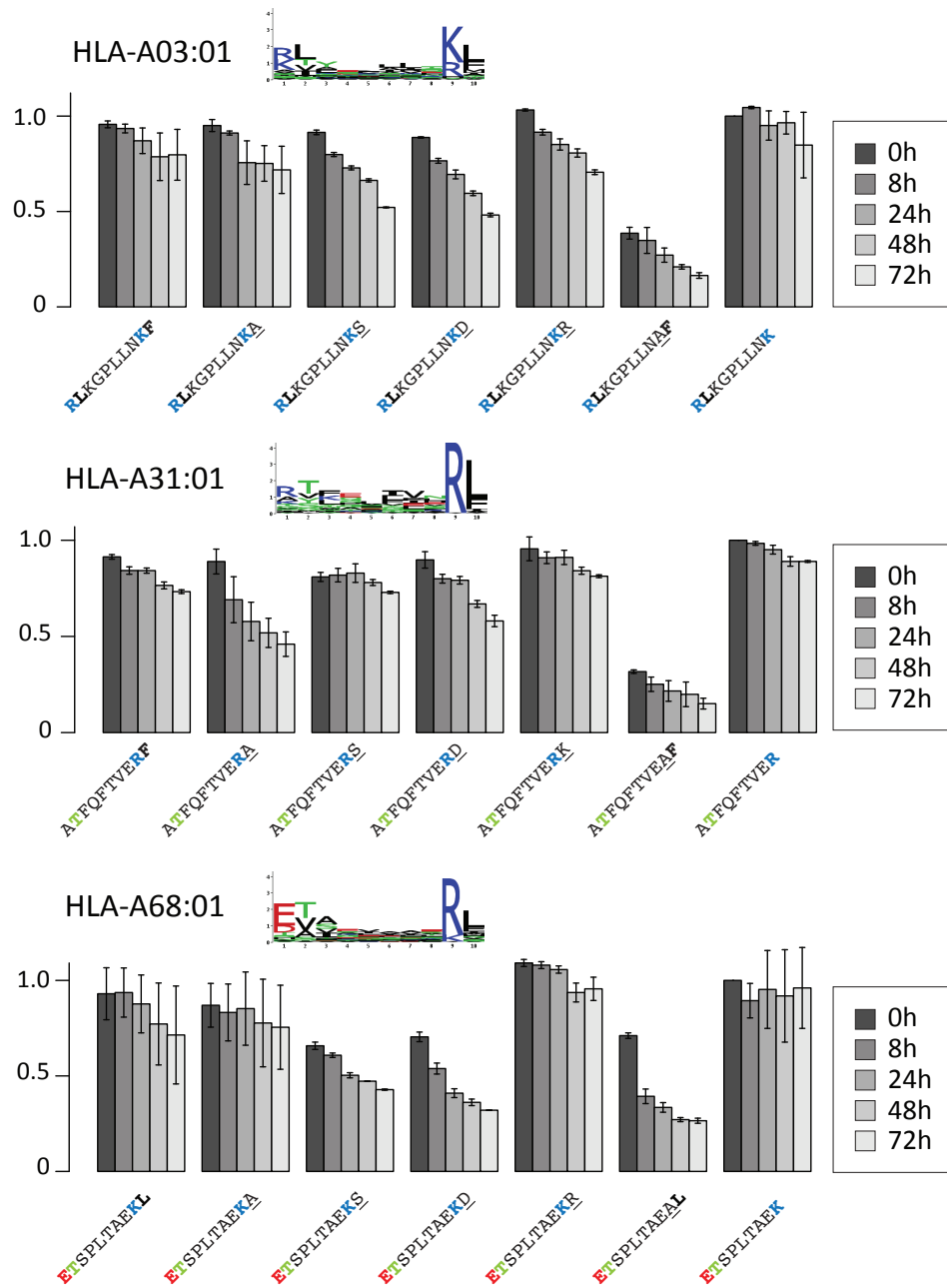


Fig. S4: Binding stability results for other P10 mutants (S,D,R/K) that did not match the specificity at P10 predicted in our analysis of MS data.

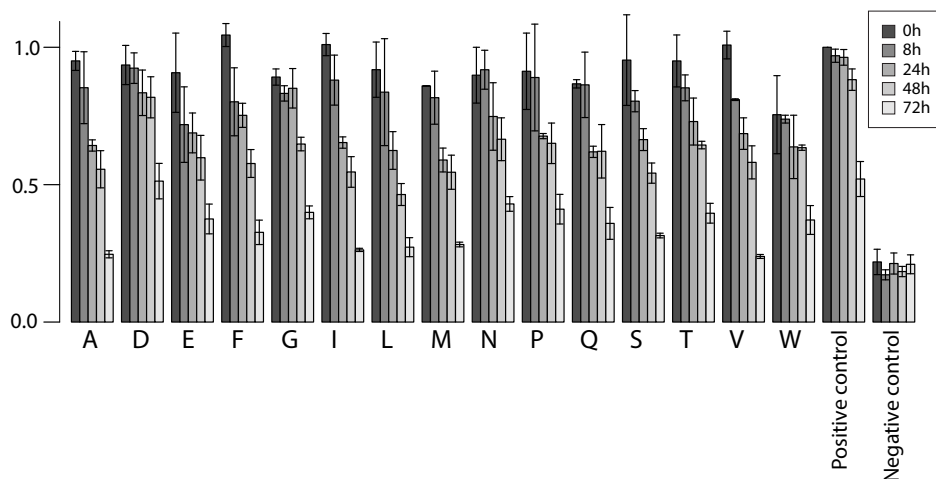


Fig. S5: Stability analysis of 11-mers built from the C-terminally extended 10-mer KLAYTLLNKL HLA-A03:01 ligand (Fig. 3) with all possible C-terminal amino acids not compatible with the specificity of the second anchor for HLA-A03:01 (i.e., KLAYTLLNKL[A/D/E/F/G/I/L/M/N/P/Q/S/T/V/W]). ILRGSVAHK was used as positive control. Negative control consists of absence of peptide.

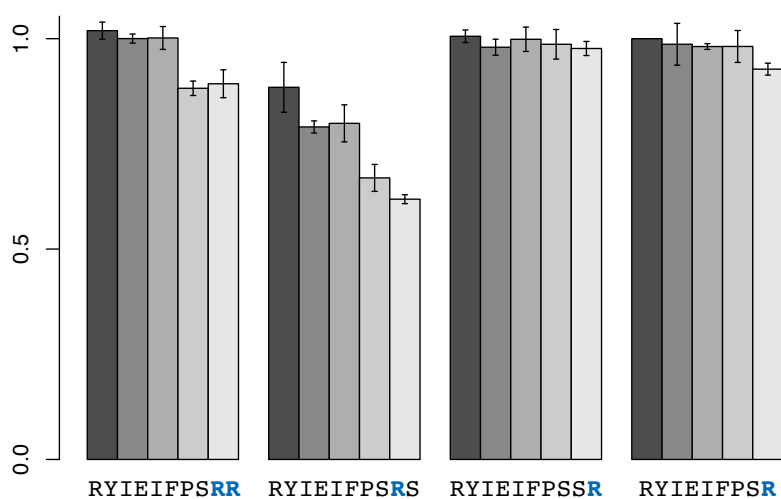


Fig. S6: Binding stability of the 10-mer RYIEIFPSRR, R(9)S and R(10)S mutants, and the 9-mer RYIEIFPSR in complex with HLA-A31:01.

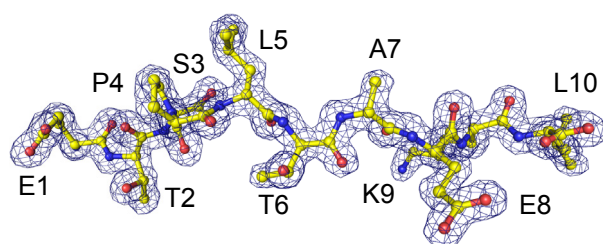


Fig. S7: Map of the peptide experimental electron density in the new X-ray structure shown in Fig. 4A (Resolution 1.6Å).

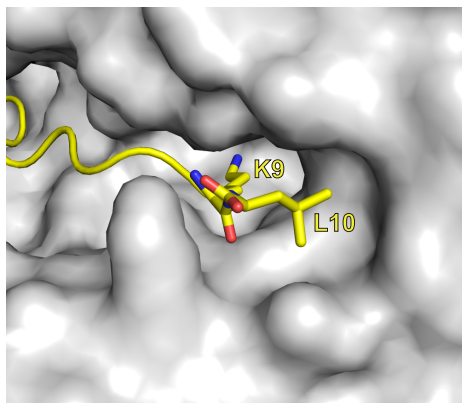


Fig. S8: Surface view of the new structure of HLA-A68:01 in complex with the C-terminally extended peptide (ETSPLTAEKL).

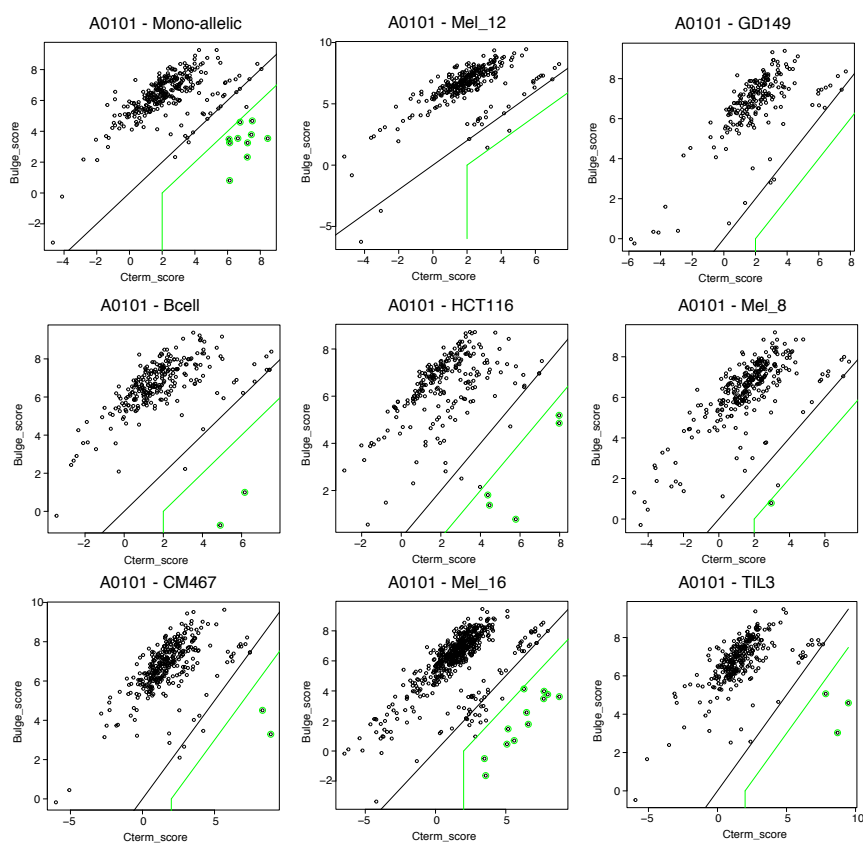


Fig. S9: Bulge versus C-terminal extension scores of peptides assigned to HLA-A0101 in the different samples where this allele is present.

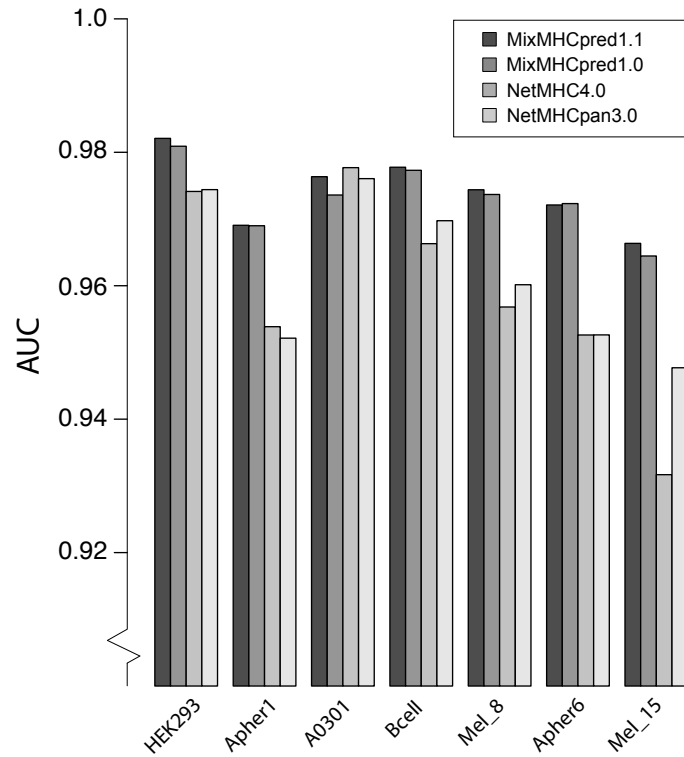


Fig. S10: AUC values for different predictors when re-predicting HLA peptidomics data from samples containing HLA-A03:01 or HLA-A68:01 alleles (same cross-validation study as in Fig. 5A).

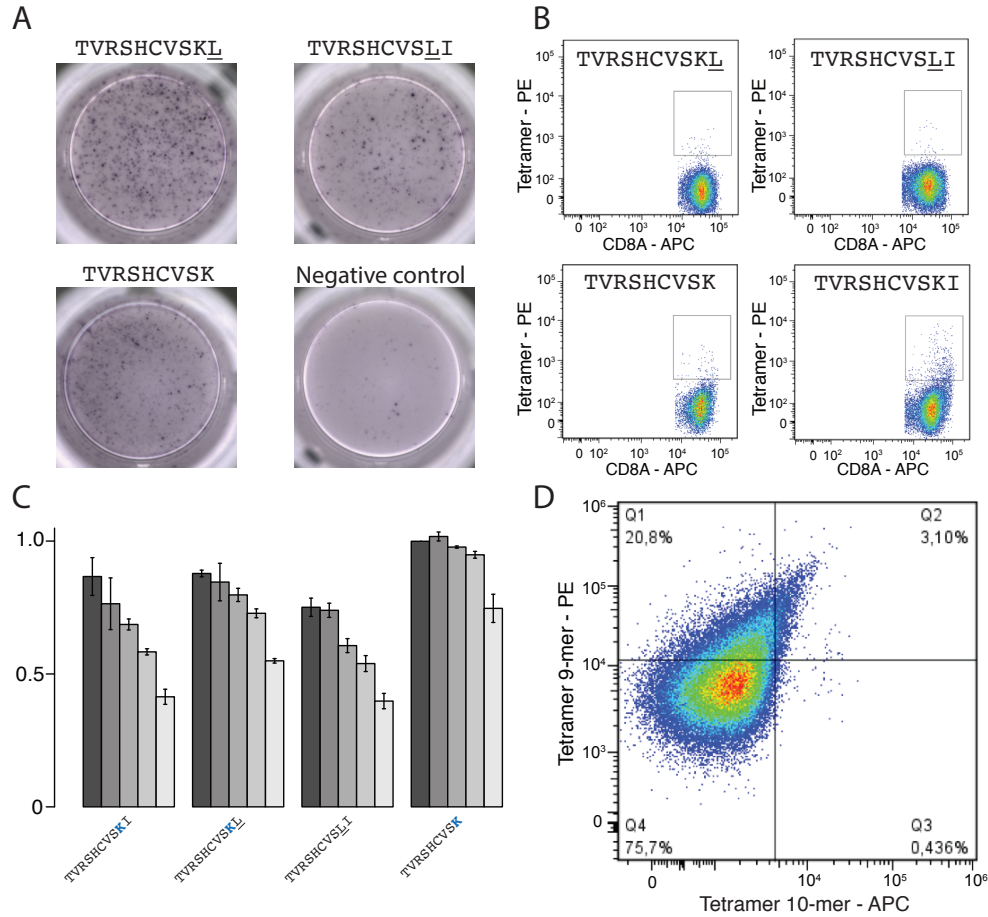


Fig. S11: A: Results of the IFN γ -ELISpot with the P10 mutant (TVRSHCVSKL), the P9 mutant (TVRSHCVSLI) and the 9-mer (TVRSHCVSK). Negative control consists of absence of peptide. **B:** Tetramer analysis with the P10 mutant (TVRSHCVSKL), the P9 mutant (TVRSHCVSLI), the 9-mer (TVRSHCVSK) and the initial 10-mer ((TVRSHCVSKI, repeats of Fig. 5D), gated on the CD8 $^{+}$. **C:** Stability analysis of the C-terminally extended CMV epitope (TVRSHCVSKI), P10 mutant, P9 mutant and the 9-mer in complex with HLA-A03:01. **D:** Cross-reactivity of TCRs binding to 10-mer (TVRSHCVSKI) with the 9-mer (TVRSHCVSK) epitope.

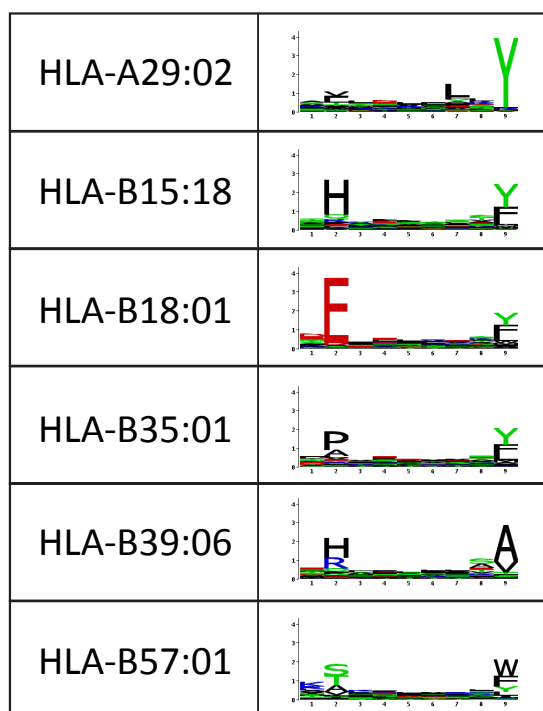


Fig. S12: Examples of alleles, together with the 9-mer motifs, for which no C-terminal extensions were observed and that do not only show preference for hydrophobic amino acids at the C-terminal anchor residue.

SI Tables

Table S1: List of X-ray structures available for alleles studied in this work. The last column shows the distance between C-alpha atoms of residues 80 and 143 (residue numbering following X-ray structures).

Allele	PDB	Resolution	Ligand	Residue at 80	Residue at 143	Distance [Å]
A01:01	3bo8	1.8	EADPTGHSY	T	T	10.1714
A02:01	2bnq	1.7	SLLMWITGV	T	T	9.99682
A02:03	3ox8	2.1	FLPSDFFPSV	T	T	10.21521
A02:07	3oxs	1.75	FLPSDFFPSV	T	T	10.20377
A03:01	3rl1	2	AIFQSSMTK	T	T	10.06951
A24:02	3vxn	1.95	RYPLTFGWCF	I	T	9.98535
A68:01	4hwz	2.4	AIFQSSMTK	T	T	10.12923
A68:02	4hx1	1.8	SVYDFVWL	T	T	10.26965
B07:02	5eo0	1.7	RPMTFKGAL	N	T	9.33824
B08:01	1m05	1.9	FLRGRAYGL	N	T	9.28667
B18:01	4xxc	1.43	DELEIKAY	N	T	9.28902
B27:04	5def	1.6	RRKWRRWHL	T	T	9.86348
B27:05	1ogt	1.47	RRKWRRWHL	T	T	10.19104
B35:01	2cik	1.75	KPIVVLHGY	N	T	9.38096
B39:01	4o2e	1.98	SHVAVENAL	N	T	9.40402
B44:02	1m6o	1.6	EEFGRAFSF	T	T	9.74925
B44:03	1n2r	1.7	EEFGRAFSF	T	T	9.8785
B51:01	1e27	2.2	LPPVVAKEI	I	T	10.26281
B57:01	5t6w	1.9	SSTRGISQLW	I	T	9.7761
C03:04	1efx	3	GAVDPLLAL	N	T	9.58623

Table S2: C-terminal extension predictions in *T. gondii* HLA-A02:01 ligands from (22).

	Number of peptides	C-terminal extension	Expected	SD	Z-score
10-mers	22	2	0.13	0.3	6.231
11-mers	25	5	0.09	0.23	21.308
12-mers	23	5	0.05	0.14	34.668

Table S3: Sensitivity of the C-terminal extension predictions with respect to different choices for the thresholds T_1 . Only alleles that passed the thresholds are shown.

$T_1=1.5$	Sample	Allele	10-mers	C-terminal Extension	Expected	SD	Z-score
Abelin	A0203	A0203	446	13	4.54	2.09	4.056
Abelin	A0207	A0207	424	17	5.06	2.12	5.629
Ritz	HEK293	A0301	1221	63	4.7	2.08	28.094
Melanoma	Mel_8	A0301	1283	25	13.21	5.04	2.34
Abelin	A0301	A0301	381	51	8.05	2.41	17.811
Melanoma	Mel_15	A0301	4865	48	13.27	4.68	7.414
Abelin	A3101	A3101	193	26	0.4	0.55	46.695
Melanoma	Mel_15	A6801	1944	38	14.18	4.74	5.026
Lausanne	RA957	A6801	4865	137	24.19	7.2	15.676
Abelin	A6802	A6802	357	11	4.36	1.68	3.957
Abelin	B5401	B5401	194	12	6.58	2.39	2.27

$T_1=2.5$	Sample	Allele	10-mers	C-terminal Extension	Expected	SD	Z-score
Abelin	A0203	A0203	446	10	2.31	1.42	5.416
Abelin	A0207	A0207	424	17	2.83	1.66	8.529
Ritz	HEK293	A0301	1221	62	0.09	0.29	212.804
Lausanne	Apher1	A0301	1273	14	2.5	1.65	6.952
Melanoma	Mel_8	A0301	1283	24	2.83	2.23	9.483
Mommen	Bcell	A0301	2521	26	5.49	2.95	6.965
Abelin	A0301	A0301	381	45	1.93	1.39	31.095
MCP	Fibroblast	A0301	859	17	2.25	1.89	7.797
Abelin	A3101	A3101	193	25	0.08	0.23	106.889
Melanoma	Mel_15	A6801	4865	136	7.65	3.25	39.49
Lausanne	RA957	A6801	1944	38	1.66	1.83	19.849
Abelin	A6802	A6802	357	10	1.57	0.96	8.736
Mommen	Bcell	B0702	2521	18	10.17	2.93	2.676
Mommen	Bcell	B2705	2521	17	6.22	2.12	5.093
Melanoma	Mel_15	B2705	4865	37	12.5	3.77	6.501
Abelin	B5401	B5401	194	12	4.56	1.94	3.842

$T_1=\text{top } 2\%$	Sample	Allele	10-mers	C-terminal Extension	Expected	SD	Z-score
Abelin	A0203	A0203	446	11	2.8	1.46	5.597
Abelin	A0207	A0207	424	17	3.64	1.9	7.037

Ritz	HEK293	A0301	1221	63	0.33	0.59	107.027
Lausanne	Apher1	A0301	1273	15	5.19	2.4	4.082
Melanoma	Mel_8	A0301	1283	25	6.73	3.74	4.891
Mommen	Bcell	A0301	2521	27	11.91	4.23	3.563
Abelin	A0301	A0301	381	48	3.28	1.85	24.142
Melanoma	Mel_15	A0301	4865	48	7.8	3.82	10.535
MCP	Fibroblast	A0301	859	17	4.69	2.76	4.464
Abelin	A3101	A3101	193	25	0.15	0.35	70.09
Lausanne	RA957	A6801	1944	38	7.06	3.12	9.932
Melanoma	Mel_15	A6801	4865	137	16.55	5.7	21.137
Abelin	A6802	A6802	357	11	1.98	1.15	7.837
Abelin	B5401	B5401	194	12	5.55	1.96	3.284

Table S4: Crystallographic data collection and refinement statistics (* Values in parentheses correspond to the highest resolution shell).

Data Collection	
PDB ID	6EI2
Protein/Ligand	HLA-A*68:01/β2M/peptide
Space group	P2 ₁ 2 ₁ 2 ₁
Cell dimensions: a, b, c (Å)	59.06 80.25 110.88
α, β, γ (deg)	90.00 90.00 90.00
Resolution* (Å)	1.61 (1.70-1.61)
Unique observations*	68846 (9873)
Completeness* (%)	99.9 (99.5)
Redundancy*	6.6 (6.6)
Rmerge*	0.094 (0.602)
I/ σI*	11.3 (2.8)
Refinement	
Resolution (Å)	1.61
R _{work} / R _{free} (%)	15.9 / 18.1
Number of atoms (protein/other/water)	3165 / 30 / 442
B-factors (Å ²) (protein/other/water)	21.85 19.95 / 33.69 / 30.45
r.m.s.d bonds (Å)	0.016
r.m.s.d angles (°)	1.714
Ramachadran Favoured (%)	97.33
Allowed (%)	2.67
Disallowed (%)	0.00

SI Datasets

Dataset S1: List of HLA peptidomics samples considered in this work with HLA typing information. Melanoma (2); MCP (1); Mommen (3); Ritz (4); Lausanne_2016 (7); Abelin (5); Hilton (6).

Dataset S2: Results of predictions of C-terminal extensions for 10-mer and 11-mer peptides. The first two columns indicate the sample of origin. Column 3 indicates the allele to which one 9-mer motif was annotated. Column 4 shows the total number of 10-mers with one-residue long C-terminal extension, respectively 11-mers with two-residue long C-terminal extensions. Column 5 shows the number of C-terminal extensions predicted for the allele in Column 3. Column 6 and 7 show the expected number and standard deviation over 100 realizations of the predicted 10-mer peptidome assuming only bulges (SI Methods). Column 8 shows the Z-score. NA stands for either motifs that could not be annotated, or cases where the number of 10-/11-mer ligands associated with the allele in column 3 did not pass our threshold (mainly B08:01 and HLA-C alleles which poorly bind longer peptides).

Dataset S3: List of 10-/11-mer peptides predicted to display C-terminal extensions for samples and alleles for which the number of C-terminal extensions passed our thresholds. These peptides were used in Fig. 2 and pooled together to define the final motifs for each allele (Fig. S2, last column).

Dataset S4: List of 10-mer peptides that had similar scores for the bulge and the C-terminal extension models in all cases predicted to display C-terminal extensions (red circles in Fig. S1).

References

1. Bassani-Sternberg M, Pletscher-Frankild S, Jensen LJ, Mann M (2015) Mass spectrometry of human leukocyte antigen class I peptidomes reveals strong effects of protein abundance and turnover on antigen presentation. *Mol Cell Proteomics* 14(3):658–673.
2. Bassani-Sternberg M, et al. (2016) Direct identification of clinically relevant neoepitopes presented on native human melanoma tissue by mass spectrometry. *Nat Commun* 7:13404.
3. Mommen GPM, et al. (2014) Expanding the detectable HLA peptide repertoire using electron-transfer/higher-energy collision dissociation (EThcD). *Proc Natl Acad Sci USA* 111(12):4507–4512.
4. Ritz D, et al. (2016) High-sensitivity HLA class I peptidome analysis enables a precise definition of peptide motifs and the identification of peptides from cell lines and patients' sera. *Proteomics* 16:1570–1580.
5. Abelin JG, et al. (2017) Mass Spectrometry Profiling of HLA-Associated Peptidomes in Mono-allelic Cells Enables More Accurate Epitope Prediction. *Immunity* 46(2):315–326.
6. Hilton HG, et al. (2017) The Intergenic Recombinant HLA-B*46:01 Has a Distinctive Peptidome that Includes KIR2DL3 Ligands. *Cell Rep* 19(7):1394–1405.
7. Bassani-Sternberg M, et al. (2017) Deciphering HLA-I motifs across HLA peptidomes improves neo-antigen predictions and identifies allosteric regulating HLA specificity. *PLoS Comput Biol* 13(8):e1005725.
8. Bassani-Sternberg M, Gfeller D (2016) Unsupervised HLA Peptidome Deconvolution Improves Ligand Prediction Accuracy and Predicts Cooperative Effects in Peptide-HLA Interactions. *J Immunol* 197(6):2492–2499.
9. Garboczi DN, Hung DT, Wiley DC (1992) HLA-A2-peptide complexes: refolding and crystallization of molecules expressed in *Escherichia coli* and complexed with single antigenic peptides. *Proc Natl Acad Sci USA* 89(8):3429–3433.
10. Kabsch W (2010) XDS. *Acta Crystallogr D Biol Crystallogr* 66(Pt 2):125–132.
11. Evans P (2017) *SCALA - scale together multiple observations of reflections*. (MRC Laboratory of Molecular Biology).
12. McCoy AJ, Grosse-Kunstleve RW, Storoni LC, Read RJ (2005) Likelihood-enhanced fast translation functions. *Acta Crystallogr D Biol Crystallogr* 61(Pt 4):458–464.

13. Perrakis A, Morris R, Lamzin VS (1999) Automated protein model building combined with iterative structure refinement. *Nat Struct Biol* 6(5):458–463.
14. Emsley P, Cowtan K (2004) Coot: model-building tools for molecular graphics. *Acta Crystallogr D Biol Crystallogr* 60(Pt 12 Pt 1):2126–2132.
15. Murshudov GN, Vagin AA, Dodson EJ (1997) Refinement of macromolecular structures by the maximum-likelihood method. *Acta Crystallogr D Biol Crystallogr* 53(Pt 3):240–255.
16. Painter J, Merritt EA (2006) Optimal description of a protein structure in terms of multiple groups undergoing TLS motion. *Acta Crystallogr D Biol Crystallogr* 62(Pt 4):439–450.
17. Robinson J, et al. (2015) The IPD and IMGT/HLA database: allele variant databases. *Nucleic Acids Res* 43(Database issue):D423–31.
18. Edgar RC (2004) MUSCLE: multiple sequence alignment with high accuracy and high throughput. *Nucleic Acids Res* 32(5):1792–1797.
19. Friedman J, Hastie T, Tibshirani R (2010) Regularization Paths for Generalized Linear Models via Coordinate Descent. *J Stat Softw* 33(1):1–22.
20. Andreatta M, Nielsen M (2016) Gapped sequence alignment using artificial neural networks: application to the MHC class I system. *Bioinformatics* 32(4):511–517.
21. Nielsen M, Andreatta M (2016) NetMHCpan-3.0; improved prediction of binding to MHC class I molecules integrating information from multiple receptor and peptide length datasets. *Genome Med* 8(1):33.
22. McMurtrey C, et al. (2016) Toxoplasma gondii peptide ligands open the gate of the HLA class I binding groove. *Elife* 5:246.